KONA Powder and Particle Journal

KONA Powder and Particle Journal No. 42 (2025) 57–78/https://doi.org/10.14356/kona.2025014 Review Paper

Integrating Flow Testing and Particle Imaging: Advances in Characterising Granular Flows †

Zohreh Farmani [1,2], Jan A. Wieringa [3], John van Duynhoven [3,4] and Joshua A. Dijksman [1,2]*

[1] *Van der Waals-Zeeman Institute, Institute of Physics, University of Amsterdam, The Netherlands*
[2] *Dept. of Physical Chemistry and Soft Matter, Wageningen University, The Netherlands*
[3] *Unilever Foods Innovation Centre, The Netherlands*
[4] *Laboratory of Biophysics, Wageningen University, The Netherlands*

In this study, we explore the intersection of mechanical testing and particle imaging techniques, offering a new perspective on granular material science. We examine a range of flow testers, such as the Schulze shear tester, FT4 powder flow tester, and split-bottom tester, each of which provides valuable insights into how materials respond to compression and shear forces. Simultaneously, we discuss imaging techniques such as refractive index matching, MRI, and X-ray imaging, revealing their capacity to capture the intricate behaviours of particles and flow dynamics at a microscopic level. This combination of macroscopic flow testing and microscopic imaging promises to unlock unprecedented insights into granular materials and complex fluids. Furthermore, we discuss the current challenges in imaging granular flows and recent advances in coupling flow tests with particle imaging.

Keywords: flow tester, particle imaging, flow dynamics, granular materials, material science

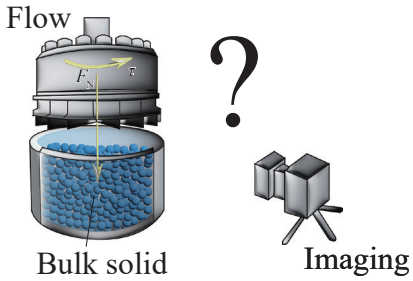

1. Introduction

Powders and granular materials are integral components in the production of everyday products, playing a pivotal role across various industrial sectors, spanning from the food industry (Cataldo et al., 2009), pharmaceuticals (Wang et al., 2016), ceramics (Curran et al., 1993), battery assembly (Gaitonde, 2016), and glue production (Duran, 2012). In these applications, the handling, flow, and compaction properties of powders and granular materials is of paramount importance. A profound understanding of their behaviour under shear and compression is indispensable for optimising industrial processes, ensuring product quality, and enhancing overall efficiency (Mesri and Vardhanabhuti, 2009). To gain such insights, one can rely on a diverse array of techniques and instruments, enabling researchers to probe the mechanical response and structural characteristics of granular materials.

In addition, particle imaging techniques have emerged as indispensable tools for understanding the dynamic behaviour of granular materials (Clarke et al., 2023), particularly due to the inhomogeneous and anisotropic flow properties exhibited by these materials. These techniques encompass a range of methodologies, including digital image correlation, particle tracking velocimetry, and X-ray tomography (Vego et al., 2022). They provide researchers with the capability to visualise and track individual particles within granular assemblies, allowing for the direct observation of important variables such as particle motion, packing density, packing structures, and flow patterns. Particle imaging techniques are particularly valuable in the context of granular material flow because they offer insights into phenomena such as particle rearrangements (Chen et al., 2021), shear banding (Wang et al., 2022a), and interparticle interactions (Wiebicke et al., 2020). By integrating mechanical testing with particle imaging, we can bridge the gap between macroscopic and microscopic observations, leading to a more comprehensive understanding of how granular materials respond to external forces.

The primary objective of flow testing is to characterise the flow behaviour of powders and granular materials—an essential facet of powder properties that requires comprehensive understanding. Flow testing involves the measurement of stress in multiple directions or planes, along with strain and flow rates. It allows for the manipulation of various experimental variables, including boundary conditions (e.g., slip, no slip, partial slip, fluidity) and rigidity (e.g., constant pressure vs. constant volume). However, selecting an appropriate flow tester presents a significant challenge because the choice depends on the specific experimental conditions, including the size constraints of the shear cell relative to the particle sizes used. Size effects also play a

† Received 17 February 2024; Accepted 15 April 2024
J-STAGE Advance published online 10 August 2024
* Corresponding author: Joshua. A Dijksman;
[1] Science Park 904, 1098 XH Amsterdam The Netherlands
[2] Helix Building, 6708 WK Wageningen, The Netherlands
E-mail: j.a.dijksman@uva.nl
TEL: +31-20-525-6311

crucial role in many flow properties; however, for very small particle sizes, the container size's impact is minimal. Nonetheless, the issue of size effects merits thorough discussion and consideration. Therefore, it is imperative to classify the various types of shear and compression testers available. Additionally, flow testers tend to become known in a particular sub-field of science and engineering, limiting the reach of the results obtained from such work.

This review paper provides a comprehensive examination of two key aspects in the study of granular materials: flow testing methodologies and particle imaging techniques. By categorising, explaining, and critically assessing these methods from a range of different fields, we aim to offer a valuable resource for researchers and engineers working in the field of granular materials. We also address the typical challenges that one might encounter in the imaging of granular materials, offering insights into how to navigate and overcome these hurdles effectively. Finally, we provide a comprehensive overview of the recent advances in imaging particulate systems. These include the following: 1) X-ray rheography, which enables the study of continuous granular flows; 2) the utilisation of multiple imaging methods, combining various techniques to align with specific research goals; 3) ultrafast electron beam X-rays, allowing for time-resolved imaging of dynamic processes; and 4) rheo-MRI, a method that has recently attracted significant attention due to its capacity to provide detailed insights into the rheological properties of a system while simultaneously offering dynamic imaging capabilities.

2. Confined flow testers

As illustrated in **Fig. 1**, flow testers can generally be categorised into two main groups: direct and indirect approaches. In direct shear testers, the direction of applied stress is not fixed, whereas in indirect methods, the applied stress remains constant, allowing for the control and direct measurement of principal stresses and deformations. The subgroups of direct methods are further divided into translational and rotational categories. In translational shear testers, relative displacement occurs in a straight-line motion, as typified by the Jenike shear tester (Jenike, 1964).

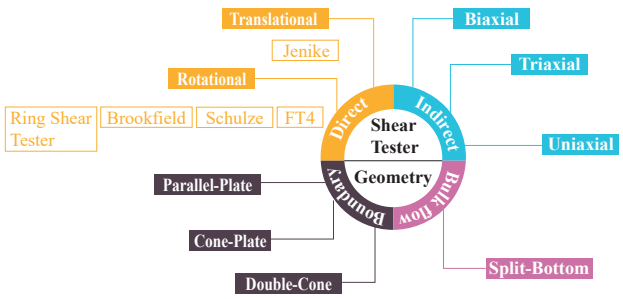

Fig. 1 Overview of existing flow testers, including direct and indirect testers and bulk and boundary flow testers.

On the other hand, rotational shear testers feature the top part of the cell rotating relative to the bottom part, and these can be further divided into torsional (Orband and Geldart, 1997) and ring shear testers (Schulze, 2011). Torsional testers involve shear deformation by rotating particles around the vertical axis, whereas ring shear testers have annular shapes that promote more homogeneous deformation (Sun, 2016). In the indirect group, testers like uniaxial, triaxial, and biaxial testers play a crucial role in studying the deformation properties of granular materials.

To study granular flows while maintaining reasonable control over boundary conditions and achieving quasi-two-dimensional flow profiles, one can turn to classical rheological geometries. Examples include parallel-plate (PP) (Lu et al., 2007), cone-plate (CP), and double-cone (DC) geometries (Tsai et al., 2020). These geometries allow for the control of shear and normal stresses on the bottom and top walls, with the imposed strain rate being independent of the radial position. Consequently, the induced flow profiles exhibit radial symmetry, at least in steady-state conditions, and even an up–down symmetry in the case of double-cone geometry when gravity can be neglected. These profiles can be accurately and relatively easily measured over a wide range of flow rates (Boyer et al., 2011; Tsai et al., 2020). Another example of such flow tests is a hopper flow tester. Extensive research has been conducted on both 2D (Wang et al., 2021) and 3D (Stannarius et al., 2019b) hopper configurations to investigate the influence of various parameters. These parameters include the hopper's height (Tsai et al., 2020), which affects the gravitational forces and pressure on the materials, and the angle of the hopper walls (Guo et al., 2023), which influences flow dynamics, the presence of an obstacle (Wang et al., 2022b), which affects the stress gradient in the packing, and the inherent characteristics of the granular material itself, such as particle size and shape (Pongó et al., 2022), friction, and stiffness (Stannarius et al., 2019a). All of these factors can significantly impact the rate and behaviour of the material as it flows through the hopper. Hoppers are also used to prepare bulk powder (e.g. in an angle of repose test). Nevertheless, we are not aware of (standardised) hopper-flow-based testers that directly quantify flow properties.

Probing the flow dynamics of granular materials presents a challenge, especially in the context of slow and fast flow limits, as defined by inertial or viscous inertial numbers (Boyer et al., 2011; Dijksman et al., 2010). For slow flows, one typically employs boundary motion, slowly shifting a container's boundary containing grains. Stress and flow profiles become independent of the flow rate, often resulting in localised shear bands near the moving boundaries. Geometries like the split-bottom Couette geometry or its variants (Dijksman and van Hecke, 2010) allow the imposition of specific flow boundary conditions

that induce wide shear zones away from boundaries. However, these flow profiles are fully three-dimensional and intricate, making it challenging to impose stress conditions. In more industrial contexts, testers designed by Jenike, Schulze, and others exhibit narrow shear zones and well-controlled stress boundary conditions (Schulze, 2008).

For faster flow limits, inclined planes (MiDi, 2004), avalanche flows (Tegzes et al., 2002), hopper flows, or impact tests (Faug, 2020) are employed. Although these setups offer access to bulk flow behaviour, they provide limited control over flow profiles and boundary conditions. Finally, rotating drum experiments, while offering good control over the overall flow rate, often exhibit intricate flow behaviour, ranging from stick-slip to highly heterogeneous flow, particularly in cohesive particle systems.

Francia et al. (2021) explored innovative techniques for characterising granular flow transitions and noted challenges in standardisation. In another review, Ogata (2019) reviewed advancements in assessing cohesive powder flowability across various handling processes.

2.1 Jenike shear tester

The Jenike shear tester is one of the earliest and most widely used powder flow characterisation techniques, originally developed around 1960 by Jenike for applications in hoppers and silos (Jenike, 1964). This shear tester simulates the flow within a hopper or silo by applying specific pressures that induce shear and consolidation of the powders.

A schematic of the Jenike tester is shown in **Fig. 2**. It consists of a fixed base part with a horizontally movable ring and a shear lid. Particles, covered with the shear lid, are placed inside the ring and the base. The testing process begins by applying a normal load to the shear lid and the particles using a weight hanger. To measure the shear force, the shear ring and lid are moved horizontally through a stem connected to a drive system. The bracket, shear lid, and shear ring transfer the measured shear force through a force transducer to the particles. Pre-consolidation is a crucial preparatory step in Jenike shear testing to establish a consistent and controlled initial state for the powders. Pre-consolidation involves subjecting the powder to a specific level of compaction or consolidation pressure before the actual shear test. This ensures that the limited shear displacement available in the tester is effectively utilised to study the material's shear behaviour without interference from inconsistent initial packing.

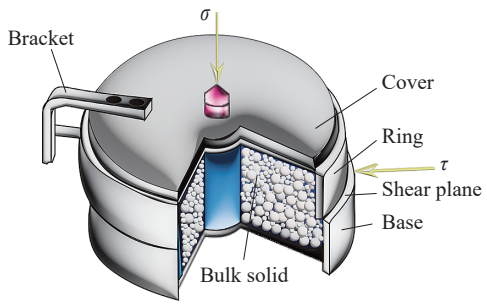

Fig. 2 Illustration of the Jenike shear tester, comprising a bracket, a stationary base section with a horizontally adjustable ring, and a shear lid by which you can impose a certain shear stress τ. The test starts by applying a normal load σ to the shear lid using a weight hanger.

Fig. 3 illustrates the stages of shear testing in the Jenike shear tester. Initially, there is a sharp increase in shear stress as time passes during the pre-shear stage. However, the curve gradually flattens until it reaches a plateau, indicating a steady-state condition. After achieving a steady state, the stem reverses, reducing the shear stress to zero. Subsequently, the stem moves forward, causing the shear stress to increase until it reaches a maximum peak. At this point, the particles begin to move and deform, leading to failure, after which the shear stress decreases.

The Jenike tester allows the measurement of parameters such as failure strength, internal friction, and wall friction (Grima et al., 2010; Han, 2011). Despite its simplicity, robustness, versatility, suitability for cohesive powders, and ability to measure wall friction, it has some limitations. The primary limitations of the Jenike shear tester are particle size (<2 mm), shear displacement (typically 6–8 mm), and small normal loads (<7 kPa) (Bilgili et al., 2004). To address these limitations, annular-shaped testers, such as the

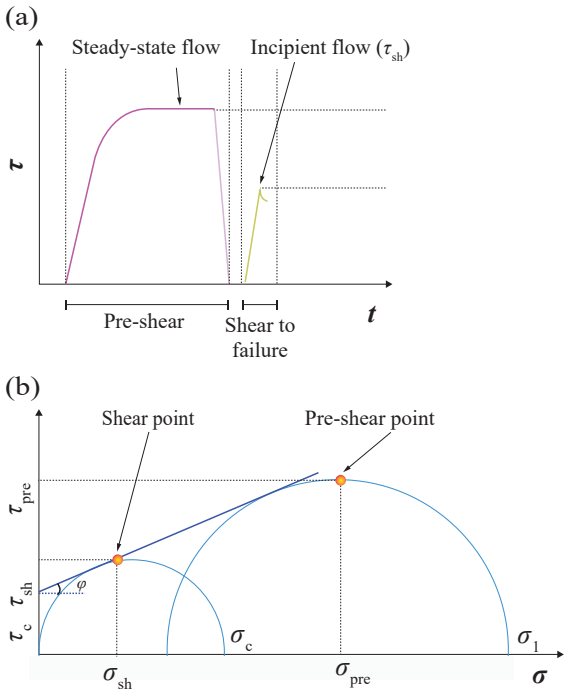

Fig. 3 **(a)** Various stages of shear testing in a Jenike shear tester, from the pre-shear phase to shear initiation and eventual failure. **(b)** Mohr circle representation, illustrating the corresponding shear point (τ_{sh}, σ_{sh}), pre-shear point (τ_{pre}, σ_{pre}), compressive strength or unconfined yield strength σ_c, consolidation stress σ_1, and angle of internal friction ϕ.

Schulze shear tester, have been introduced (Schulze, 2008). These testers offer improved capabilities for studying powders under specific conditions and have become valuable tools in powder flow research.

2.2 Schulze shear tester

The Schulze shear tester, depicted in **Fig. 4**, features an annular design in which particles are placed within an annular bottom ring of the shear cell. An annular lid attached to a crossbeam covers the particles from above. To measure the shear force, two parallel tie rods are connected to a load beam, allowing for the measurement of forces acting on the tie rods. The shearing test starts by rotating the bottom ring in a specific direction, with the tie rods preventing any rotation in the crossbeam and lid. Similar to the Jenike tester, a normal load is applied using a weight hanger attached to the crossbeam. Unlike the Jenike tester, where preconsolidation is required (due to limited shear displacement), the Schulze shear tester eliminates this need. After inserting the weight hanger, counterweight system, and tie rods on the crossbeam, the cell is ready for the shearing test. The steps involved in conducting the experiments are illustrated in **Fig. 5**. During the pre-shearing phase, the shear stress increases with time until it reaches a maximum value. Subsequently, in the steady state, the rotation direction is reversed until the shear stress drops to zero. The next shearing step continues until another maximum shear stress, indicating particle flow (failure), is achieved. Testing can proceed further by repeating the pre-shearing and shearing stages until another failure point is reached.

Two versions of the Schulze tester are currently available: the shear cell XS with a specimen volume of 30 cm^3 (RST-XS) and the shear cell M with a specimen volume of 900 cm^3 (RST-M). In 2008, a "round robin" project was initiated to investigate ring shear testers (Schulze, 2011). The primary objective of this round robin project was to establish a range of results for specified bulk solid, specifically limestone powder CRM-116. This initiative aimed to create a reference range of results, similar to what had been accomplished with the Jenike shear tester (Akers, 1992). This reference range serves as a benchmark, enabling users to assess whether their testing equipment can yield results that align with the established reference values. The round robin study also provides recommendations for the operational conditions of the Schulze tester.

The Schulze shear tester has been widely used in various research works focussed on powders and granular materials. Researchers have employed Discrete Element Method (DEM) simulations to replicate powder flow in this tester (Guo et al., 2019). These simulations, conducted with spherical and elongated particles, serve to calibrate the parameters influencing shear flow. Key parameters, including particle shape, particle stiffness (Coetzee and Els, 2009), shear cell size (Aigner et al., 2013), shear rate, Poisson's ratio, and coefficient of restitution (Wang et al., 2020), and particle–wall friction coefficient (Simons et al., 2015) were evaluated through shear tester simulations.

The Schulze shear tester offers several advantages over the Jenike shear tester, such as low and negative normal forces (<100 Pa), delicate materials, adjustable lid (more uniform shear distribution), lightweight design, unlimited shear displacement and strain, and particle size (up to

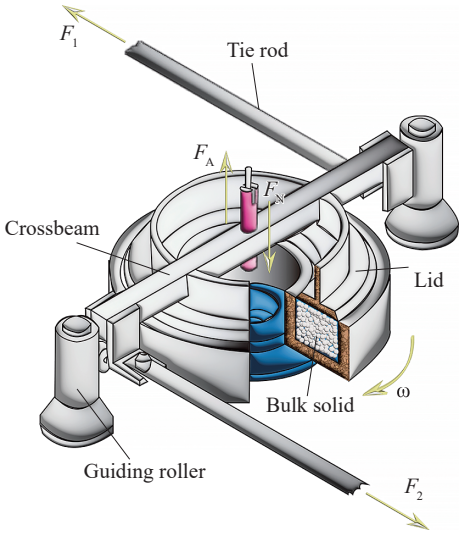

Fig. 4 Illustration of the Schulze shear tester, comprising an annular bottom ring, annular lid, crossbeam, two parallel tie rods (measuring two acting forces F_1 and F_2), load beam, and guiding rollers. Shear force τ is equal to $F_1 + F_2$. A normal load σ is applied using a weight hanger attached to the crossbeam.

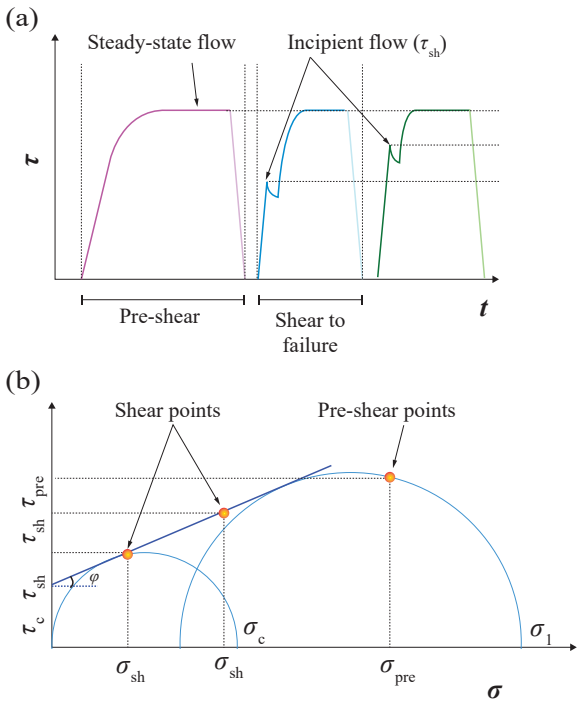

Fig. 5 Various stages of shear testing in a Schulze ring shear tester. **(b)** Mohr circle representation.

5 mm). For very fine or very coarse materials, alternative testing methods may be required.

Although the Schulze shear tester is versatile, it may not be ideal for all types of materials. It is particularly well suited to bulk solids and dry powders. Materials with unique properties, such as highly-cohesive particles, may pose challenges in the testing and interpretation of results. Similar to many other testing methods, the Schulze shear tester may be sensitive to temperature and moisture levels. Variations in environmental conditions, such as temperature and moisture level can impact material behaviour during testing.

2.3 FT4 shear tester

In 2003, Freeman Technology, a company based in Tewkesbury, UK, introduced the FT4 powder tester (Freeman, 2004). Originally intended for characterising the rheological properties of powders, this tester has evolved to cover a broad spectrum of applications. Over time, it has incorporated various accessories and methodologies, categorising it into bulk (density, compressibility, and permeability), dynamic flow (flowability, aeration, consolidation, flow rate, and specific energy), shear (shear cell, and wall friction), and process (segregation, attrition, caking, electrostatics, moisture, and agglomeration) testing capabilities. This versatility has resulted in a substantial body of work employing this shear tester (Hare et al., 2015; Khala et al., 2021).

The FT4 tester combines rotational and translational testing principles. It features a twisted blade that rotates and moves vertically downward and upward through the powder bed. A schematic of the FT4 tester is shown in **Fig. 6**. The testing procedure involves four key steps: conditioning, consolidation, pre-shearing, and shearing, which closely mirror the procedures of other shear testers. Upon filling the glass cell, the blade initially descends to compress the powder bed. It then ascends to remove excess powder from the surface, creating a homogeneous layer—a process similar to that of the Schulze tester. Notably, the FT4 tester incorporates an automated conditioning mode, distinguishing it from other testers that require manual intervention with a spatula.

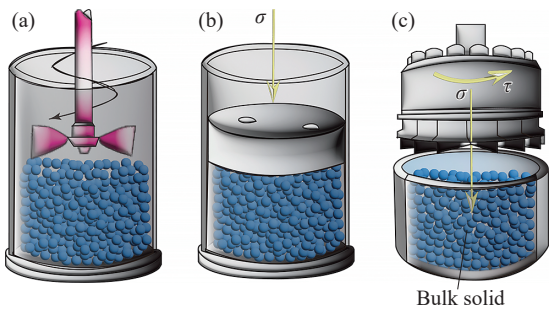

Fig. 6 Schematic of the FT4 shear tester. **(a)** A twisted blade rotates vertically downward and upward (torque and force can be measured), **(b)** a vented piston can consolidate the powder under a controlled normal stress σ, and **(c)** an automated rotational shear cell accessory that can go inside the packing and rotate.

During the testing procedure of the FT4 tester, after the conditioning step, a specific normal stress σ is applied during the consolidation step. Subsequently, the pre-shearing and shearing steps follow, analogous to the procedure illustrated in **Fig. 5** for the Schulze tester. This entire sequence can be repeated multiple times (typically 3 to 5) to enhance the accuracy and reliability of the results.

The FT4 shear tester is a versatile and comprehensive powder tester that covers a broad range of testing methodologies and parameters, including powder flowability, air flow (Nan et al., 2017b), particle shape (Nan et al., 2017a), dynamic flow behaviour (Hare et al., 2015; 2017), shear characteristics (Hare and Ghadiri, 2017), and various process-related attributes. In addition to the extensive volume of powder rheometry experiments conducted with FT4, a body of numerical research complements the experimental work (Khala et al., 2021; Nan and Gu, 2020).

The FT4 tester typically operates within a maximum consolidation normal stress of 3–7 kPa, maximum torque of 900 mN·m, and maximum rotational and axial speeds of 120 rpm and 30 mm/s. The FT4 tester may not be suitable for powders with large particle sizes. Its maximum particle size capability is around 1 mm, which is smaller than that of some other shear testers like the Schulze tester (up to 5 mm). This limitation may affect its applicability to coarser materials (Cordts and Steckel, 2012). In comparison with certain other shear testers, the FT4 tester measures a moderate range of shear stresses. This limitation means that it may not be an ideal choice for materials requiring very high shear stresses for characterisation.

2.4 Brookfield powder flow tester

In 2009, a powder flow tester emerged through collaborative efforts between the Wolfson Centre for Bulk Solids Handling Technology at the University of Greenwich and certain private food manufacturers. The tester garnered attention for its ease of use and broad applicability (Berry et al., 2015). While this tester's design principles align with those of the Jenike tester, their primary distinction lies in their intended purpose, which is to tailor it for quality control applications. Numerous studies in the literature (Salehi et al., 2017) have now showcased industrial trial results and affirmed the applicability and utility of the Brookfield powder flow tester.

Fig. 7 illustrates the Brookfield setup, including the flow function lid and trough filling accessories. Notably, the Brookfield tester incorporates an annular shear cell, similar to the Schulze tester. However, it is different in its design, where the lid attaches to the compression plate, facilitating powder filling and load application with minimal operator involvement. The simplicity of conducting powder

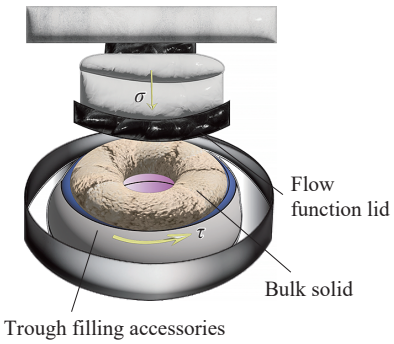

Fig. 7 Schematic of the Brookfield shear tester including the annular shear cell, flow function lid, and trough filling accessories.

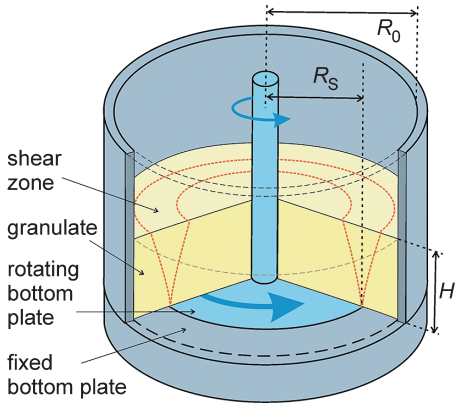

Fig. 8 A schematic of the split-bottom shear cell, with R_s the radius of the inner cylinder, R_o the radius of the outer cylinder, and H the thickness of the particle layer. (Reprinted from Ref. (Wang et al., 2022a) under the terms of the CC-BY 4.0 license. Copyright: (2022) The Authors, published by Springer Nature.

rheology tests with Brookfield equipment has recently made it a popular choice (Leaper, 2021; Navar et al., 2022).

The Brookfield tester facilitates the measurement of several key parameters, including flow function, unconfined failure strength, time consolidation, internal friction angle, cohesion, wall friction, bulk density, and compressibility. In terms of the shear stress they measure, a comparison reveals that the Brookfield tester measures moderate shear stresses compared to the Jenike and Schulze testers, where Jenike < Brookfield < Schulze.

However, like its counterparts, the Brookfield tester is not without limitations. Its primary constraint pertains to the maximum consolidation normal stress (4.8–13 kPa), which is much lower than that of the Schulze shear tester (50 kPa). Regarding the particle size that it can accommodate, one can consider Brookfield < Jenike < Schulze. This implies that the Brookfield tester is most suitable for materials with particle sizes up to approximately 1 mm, which is considerably smaller than the maximum particle sizes accommodated by the Jenike (2 mm) and Schulze (5 mm) testers.

3. Unconfined flow testers

3.1 Split-bottom shear tester

In granular flow, the tendency towards localisation in narrow shear bands is a common phenomenon (Szabó et al., 2014; Unger et al., 2004), but there are instances, particularly in slow granular flows, where wider shear zones can be observed (Dijksman and van Hecke, 2010; Fenistein and van Hecke, 2003). To generate slow flows with distinct shear bands, researchers have proposed the use of split-bottom geometry (Fenistein et al., 2004; Wang et al., 2022a). This configuration involves splitting the bottom part of a concentric cylinder system into two sections that can slide past each other, offering greater stability to the shear bands at fixed positions.

Fig. 8 presents a schematic of the split-bottom geometry. By rotating the inner part, a shear zone is observed to propagate upward and inward from the slip position. The split-bottom cell's unique geometry allows for investigating various factors beyond flow transitions in slow granular flows. These factors include suspension and granular flows (Shaebani et al., 2021; Singh et al., 2014; Wang et al., 2022a), segregation mechanisms (Gillemot et al., 2017), fluid depletion (Mani et al., 2012), non-local flows (Henann and Kamrin, 2013), and faster flows (Luo et al., 2017).

In addition to the experimental investigations, the split-bottom shear cell is often used in numerical simulations, particularly either in Finite Element Method (FEM) simulations (Henann and Kamrin, 2013) or Discrete Element Method (DEM) simulations (Luding, 2007). The geometry of the split-bottom shear cell provides a well-defined boundary condition and initial configuration for FEM and DEM simulations, making it an excellent choice for calibration.

Despite the above-mentioned advantages of the split-bottom geometry, there are some limitations. The limitations of a split-bottom shear cell include constraints related to particle size compatibility (100 μm to a few mm), the range of applicable confining stresses (0.1–2 kPa), and the absence of features for precise temperature or environmental control. Thus far, the flow geometry has not been used in any commercially available or standardised testing machine.

3.2 Rotating drum

In addition to traditional shear testers, a rotating drum is another valuable tool for studying the behaviour of granular materials. This dynamic testing system, originally introduced by Yuri Oyama (1940) in 1940, has gained significant attention from researchers interested in granular material dynamics. It has proven to be an effective method for investigating mixing and segregation, which are fundamental processes in various industrial applications.

Researchers have conducted numerous experiments (Huang et al., 2021; Li et al., 2021) and theoretical (Li et

al., 2021; Xiu et al., 2021) studies using rotating drums, exploring various parameters that affect granular material behaviour. These parameters include particle shape (Preud'homme et al., 2021), drum geometry (Fiedor and Ottino, 2003), filling ratio (Inagaki and Yoshikawa, 2010), and segregation mechanisms (Chen et al., 2010).

A typical rotating drum setup, depicted in **Fig. 9**, consists of a cylindrical vessel with specific dimensions that can rotate at an angular velocity ω. The drum is partially filled with particles, although fully filled drums have been studied under specific conditions (Inagaki and Yoshikawa, 2010).

The testing procedure for rotating drum involves partially filling the drum with particles. The drum is then rotated at a controlled angular velocity ω. As the drum rotates, various flow regimes are observed (Yang et al., 2008), depending on the rotational speed, including slipping at low ω, slumping, rolling, cascading at intermediate ω, and cataracting and centrifuging at high ω. Researchers typically focus on rolling regimes, which are relevant to many industrial processes. Throughout the experiment, parameters such as particle motion, segregation, mixing behaviour, and the angle of repose, which defines the maximum angle at which a granular material remains stable on a surface, were closely monitored and analysed.

Rotating drum allows for the visualisation of the flow regime transitions, segregation, and mixing efficiency (Beaulieu et al., 2022). The velocity profiles of particles in the drum can be measured to gain insights into the distribution of particle speeds during mixing. Moreover, one can measure a (dynamic) "angle of repose" that provides information about its flowability and internal friction. Parameters like the flowability index ($\frac{\rho_{Tapped}-\rho_{Bulk}}{\rho_{Tapped}}$) or the Hausner ratio ($\rho_{Tapped}/\rho_{Bulk}$) can be determined to assess the flow properties of granular materials. The drum can also be used to study how particle shape influences segregation, mixing, and flow patterns (Cunez et al., 2023; He et al., 2023).

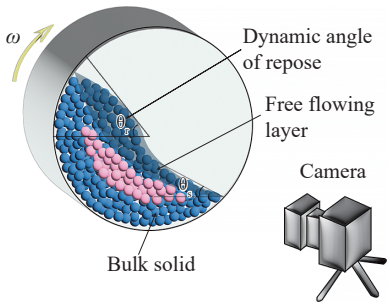

Fig. 9 Schematic of a rotating drum consisting of a cylindrical vessel rotating at an angular velocity ω. The drum is partially filled with particles. By visualising the particle motion through a camera, one can measure the dynamic angle of repose θ.

4. Compression testing techniques

4.1 Uniaxial compression tester

A schematic of the uniaxial compression cell is depicted in **Fig. 10**. The uniaxial compression test procedure is similar to that of the Jenike shear tester (Parrella et al., 2008). A sample is filled into a cylinder with frictionless walls and is consolidated under a normal stress σ_1 (consolidation stress), leading to an increase in bulk density ρ_b (Cavarretta and O'Sullivan, 2012). This consolidation step is the same as the pre-shear step in shear testers. After removing the cylinder, the sample is loaded vertically with an increasing normal stress up to the point of failure, where the sample will experience a break or failure at a certain stress σ_2. The stress at failure is the unconfined yield strength. Contrary to the results of the shear tests, steady-state flow cannot be reached during consolidation. By reaching the failure point, the sample begins to flow. Uniaxial compression tests can be conducted at different consolidation stresses, allowing us to plot the unconfined yield strength against the consolidation stress. This produces a flow function curve, as illustrated in **Fig. 11**, which aids in assessing the sample's flowability. In order to characterise the flowability, the term ff_c is defined as the ratio of consolidation stress σ_1 to

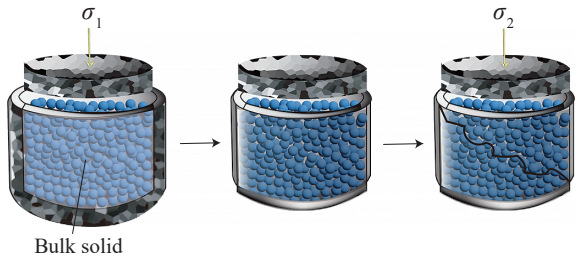

Fig. 10 Steps of the uniaxial compression test. The first step **(left)** is the consolidation of particles inside the cylinder under a normal stress σ_1. In the next step, we remove the cylinder. At the final step **(right)**, the particles will experience a failure at a certain stress σ_2 called unconfined yield strength.

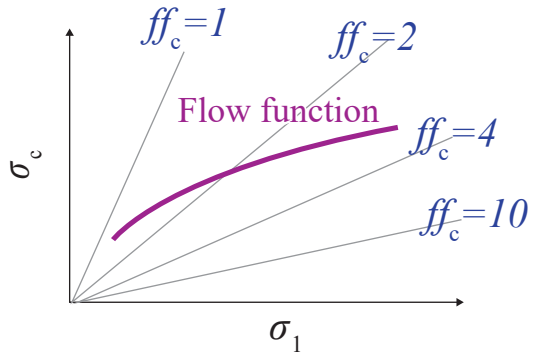

Fig. 11 Flowability curve: unconfined yield strength σ_c versus consolidation stress σ_1. The term $ff_c = \sigma_1/\sigma_c$, characterises the flowability of particles. The larger the ff_c is, the better the particle flow. There are five regions in the flowability curve: no flowing ($ff_c < 1$), very cohesive ($1 < ff_c < 2$), cohesive ($2 < ff_c < 4$), easy-flowing ($4 < ff_c < 10$), and free-flowing ($ff_c > 10$).

unconfined yield strength σ_2. The larger the ff_c is, the better the particle flow. In **Fig. 11**, you can find a flowability classification close to the Jenike classification, which specifies that under higher consolidation stress, a particle can flow better.

4.2 Biaxial compression tester

The biaxial tester can be considered as a translational tester because it consists of two movement in x and y directions. As can be observed from **Fig. 12**, there is a loading plate, loading rod, and guide rod by which the test can be performed. In the first step after filling the cell with particles, the loading plate, which is placed on top of the base cell, moves through x direction until the favourable consolidation stress σ is gained. By moving this plate, the particles are consolidated. In order to obtain a constant consolidation stress and reach a steady-state flow, the loading plate can be pushed further in x direction and at the same time, the guide rod will move backward in y direction. After the steady-state step, there is an unloading step in both x and y directions. To measure the unconfined yield strength, the guide rod should first be removed, and then the loading plate moves again in x direction until failure occurs. The unconfined yield strength can be calculated from the force acting on the loading rod at failure. The similarity between uniaxial and biaxial tests is in the application of consolidation stress and measurement of the unconfined yield strength (Satone et al., 2017).

4.3 Triaxial compression tester

This tester is the standard shear tester in soil mechanics (Balla, 1960; Oda, 1972), and is mostly applicable for the measurement of shear strength, cohesion, permeability, and stiffness (Schnaid et al., 2001; Shinohara et al., 2000). For testing, the sample must be placed in a cell that can be pressurised and sealed with a rubber membrane along its walls. The rubber membrane must be pre-stressed; therefore, the tester in its standard form is not applicable to the low-stress region of interest in powder technology. After filling the cell with particles, the particles are usually, but not always, saturated, consolidated, and sheared. During the shearing step, the particles are loaded axially, which can be by compression or extension. Based on the schematic of the triaxial setup shown in **Fig. 13**, the triaxial cell is placed inside a pressure vessel. By pressing the fluid surrounding the cell, the confining pressure σ is applied. The triaxial cell is placed between a loading platform from the bottom, which can move upward, and a loading cell on the top. There is also a hydraulic unit to control the cell pressure. Vacuum is used to hold the particles inside the cell until the confining pressure is applied. The entire setup is connected to a computer system to record the transducer data of displacement, pressure, and force.

Within the domain of granular materials, researchers frequently employ triaxial tests to examine a diverse array of mechanical properties and behaviours exhibited by these materials under carefully controlled conditions. Triaxial tests also have substantial utility in the field of experimental granular physics, where they serve as valuable tools for delving into the fundamental (anisotropic) mechanical characteristics and behaviours inherent to granular materials. Such investigations provide valuable insights into intriguing phenomena, including jamming (Peshkov and Teitel, 2022), shear localisation, and the dynamics of granular flow (Nadimi et al., 2020). Additionally, noteworthy studies have explored the application of triaxial tests to the rheology of soft particles (Nezamabadi et al., 2021; Vu et al., 2021), further expanding the scope of research in this area.

Note that beyond the aforementioned flow testers, the capillary flow tester has been employed to optimise manufacturing processes and ensure product quality of particles

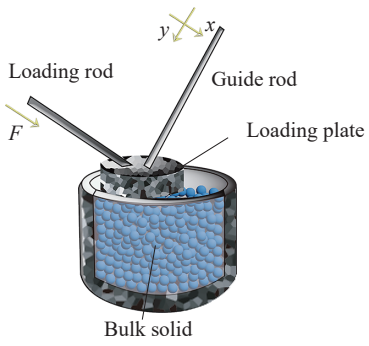

Fig. 12 Schematic of biaxial tester including a loading plate, loading rod, and guide rod. By moving the loading plate until a certain consolidation stress σ, the particles are consolidated. The unconfined yield strength can be calculated from the force F acting on the loading rod at failure.

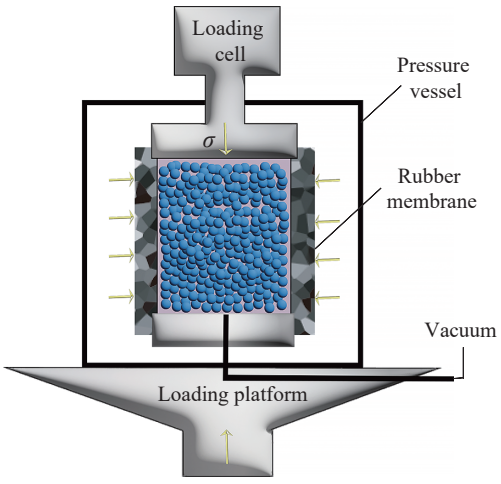

Fig. 13 Schematic of triaxial tester including the loading cell, loading platform, pressure vessel, rubber membrane, and vacuum. The triaxial cell is placed between a loading platform from the bottom and a loading cell on the top. A hydraulic unit controls the cell pressure, while vacuum holds particles until confining pressure σ is applied.

in industrial processes, albeit at limited scale so far for particles or particle-fluid mixtures. The capillary flow tester focuses on the fluid or ductile material's behaviour as it flows into and within a capillary. Typically, the pressure difference along the capillary is measured in relation to the material flow rate, allowing the extraction of specific rheological information from this data (Mackley and Rutgers, 1998), especially at elevated pressures. Utilising a capillary flow tester, or capillary rheometry, offers the advantage of efficiently accessing high shear rate flow properties and flow instabilities relevant to industrial processing. Capillary rheometry has found application in simulating polymer extrusion processes (Couch and Binding, 2000; Laun, 2004), food processing (Zhang et al., 2022), coatings production (Luo et al., 2021), and pellet manufacturing (Bastiaansen et al., 2023).

5. Comparison of confined and unconfined flow testers

We have summarised the advantages, limitations, and applications of the various powder testers in **Tables 1** and **2**. Extensive research has been conducted to compare the functionality and applicability of these powder rheometry methods. These studies encompass comparative analyses of flow properties in cohesive powders (Du et al., 2023; Koynov et al., 2015; Leturia et al., 2014; Salehi et al., 2017; Shi et al., 2018; Zafar et al., 2019), pharmaceutical powders (Deng et al., 2022; Leaper, 2021; Shah et al., 2008; Tay et al., 2017), steel powders (Marchetti and Hulme-Smith, 2021), and food powders (Juliano and Barbosa-Cánovas, 2010).

6. Particle imaging methods

Imaging of particle systems is highly valuable because it provides visual insights into the behaviour and interactions of individual particles within a larger assembly. This enables researchers to observe microscopic details, analyse flow dynamics, track changes over time, and bridge micro (particle) and macro (constitutive modelling) levels. Imaging techniques have been combined with rheometry or particle flow measurements in various systems to gain a comprehensive understanding of the material behaviour (Amon et al., 2017). In the study of granular materials, imaging techniques such as high-speed cameras, X-ray imaging, and laser-based imaging methods have been integrated with rheometers to perform rotational shear and compression measurements. This combination allows simultaneous measurement of the rheological properties of the particles under shear or compression and visualise the particle flow and interactions in real time. In addition to granular materials, the combination of imaging with flow measurements has been used in complex fluids, such as emulsions (Paredes et al., 2011), suspensions (Graziano et al., 2021; Moud et al., 2022), and foams (Verma et al.,

Table 1 Comparison of different shear and compression testers.

Tester	Advantages	Limitations	Typical applications
Jenike (Jenike, 1961)	Simplicity and robustness; Historical significance.	Limited shear displacement (6–8 mm); Normal loads (>7 kPa); Particle size <2 mm; Stress homogeneity.	Design of silos for flow (Schwedes, 2003); measurement of failure strength and wall friction (Han, 2011).
Schulze (Schulze, 2008)	Unlimited shear displacement; Low or negative normal forces possible (<100 Pa); Uniform shear distribution.	Particle size <5 mm; Not suitable for highly cohesive and highly elastic powders.	Measuring shear strength, flow function ff_c, angle of internal friction ϕ, wall friction, bulk density ρ_b (Schulze, 2021; Wang C. et al., 2022).
FT4 (Freeman, 2004; 2007)	Originally designed for rheology; Versatile and comprehensive; Addresses diverse needs in research and industry.	Limited maximum consolidation normal stress (3–7 kPa); Particle size <1 mm; Not suitable for extremely elastic/coarse powders.	Bulk (density, compressibility, and permeability) (Nkurikiye et al., 2023); Dynamic flow (flowability, aeration, consolidation, flow rate, and specific energy) (Divya and Ganesh, 2019); Shear (shear cell, and wall friction) (Hare and Ghadiri, 2017) ; Process (segregation, attrition, caking, electrostatics, moisture, and agglomeration) (Mitra et al., 2017).
Brookfield (Berry and Bradley, 2010)	Fast, economical, and easy to use; product improvement and quality control.	Limited maximum consolidation normal stress (4.8–13 kPa); Particle size <1 mm, Not for extremely elastic bulk solids.	Measuring flow function, unconfined failure strength, time consolidation, angle of internal friction ϕ, wall friction, bulk density ρ_b, compressibility (Navar et al., 2022).

Table 2 Comparison of different shear and compression tests.

Tester	Advantages	Limitations	Typical applications
Split-Bottom (Fenistein et al., 2004; Fenistein and van Hecke, 2003).	Robust shear bands; Can be easily coupled with 3D imaging techniques.	Limited control over complex industrial flow conditions; Not suitable for powders due to split geometry; Only for quasi-static flows.	Dense suspensions and slow granular flows (Wang et al., 2022a), segregation (Gillemot et al., 2017); fluid depletion (Mani et al., 2012), non-local flows (Henann and Kamrin, 2013); faster flow (Luo et al., 2017).
Rotating Drum (Oyama, 1940)	Studying mixing and segregation; Visualisation of flow regime transition.	Limited control over complex industrial flow conditions.	Fundamental research on granular materials; Measuring dynamic angle of repose, flowability, and internal friction (Huang et al., 2021; Li et al., 2021).
Uniaxial	Measures compressive strength under 1D compression; Simple and widely used.	Limited to 1D compression tests and fine-grained/cohesive powders; Cannot measure internal or wall friction.	Basic assessment of compressive behaviour in granular materials (Cheng and Wang, 2022; Le, 2022) and flowability.
Biaxial	Measures compressive strength under confined conditions.	Limited to confined compression tests.	Study of confined compression behaviour in granular materials (Satone et al., 2017).
Triaxial	Measures compressive strength under controlled confining pressure.	Requires complex testing equipment.	Soil mechanics (Oda, 1972) (measurement of shear strength, cohesion, permeability and stiffness (Schnaid et al., 2001)).

2018). For example, particle tracking velocimetry (PTV) or particle image velocimetry (PIV) techniques combined with rheological measurements provide insights into the microstructure, particle dynamics, and flow behaviour of these complex fluid systems.

We review several common approaches that stretch the limits of particle imaging-based techniques. These techniques provide insights into the behaviour, properties, and dynamics of granular systems. They allow us to unravel the fundamental principles governing the behaviour of granular materials, such as their flow patterns, packing structures, particle rearrangements, and interparticle interactions. Furthermore, these methods extend their reach beyond granular materials alone.

6.1 Optical techniques

6.1.1 Optical microscopy

Optical microscopy (OM) is a widely used technique for studying particle flow fields (Wang et al., 2022b). **Fig. 14** shows a schematic representation of the optical microscope. OM involves the use of visible light to observe and analyse the behaviour, properties, and dynamics of particles. It requires a light source, typically a lamp or laser, to provide illumination. Light passes through or reflects off the particles of interest. Proper sample preparation, including mounting and positioning, ensures adequate interaction of the light with the particles. The light transmitted or reflected by the particles is collected by an objective lens, which focuses on the light onto an image plane or an eyepiece. The lens system provides magnification, allowing for detailed visualisation of the particles and their interactions. The focussed light forms an image of the particles on a detector, which can be a camera or the human eye. The captured images are then analysed using various techniques, such as image processing, particle tracking

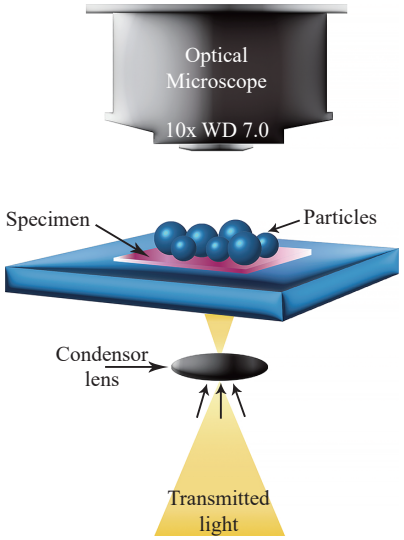

Fig. 14 Schematic of optical microscopy (OM) including a light source and a condenser lens.

algorithms, and manual measurements, to extract relevant information about particle size, shape, packing arrangements, and flow behaviour.

6.1.2 Confocal microscopy

Confocal microscopy (CM) is a powerful imaging technique used to study colloidal suspensions (Hooiveld et al., 2023; Rathee et al., 2020), Pickering emulsions (Benyaya et al., 2023), fluid flow and particle dynamics in microfluidic devices (Lochab et al., 2019), inkjet printing (Shi et al., 2021) and more. It provides high-resolution three-dimensional imaging by selectively focussing on a specific plane within the sample while rejecting out-of-focus light. **Fig. 15** shows a schematic of the confocal microscope. CM uses a laser as the light source. The laser beam is directed onto the sample, and the light emitted from the particles is collected. A pinhole aperture is placed in front of the detector to block out-of-focus light. This pinhole allows only the light emitted from the focal plane to pass through, ensuring that only in-focus information is captured. The laser beam is scanned across the sample using a scanning system such as a galvanometer mirror or acousto-optic deflector. This scanning mechanism rapidly moves the focal point of the laser through the sample in a predefined pattern. The emitted light passes through the pinhole and is detected by a sensitive photodetector, such as a photomultiplier tube or avalanche photodiode. The detected signal is then used to reconstruct a two-dimensional or three-dimensional image of the sample.

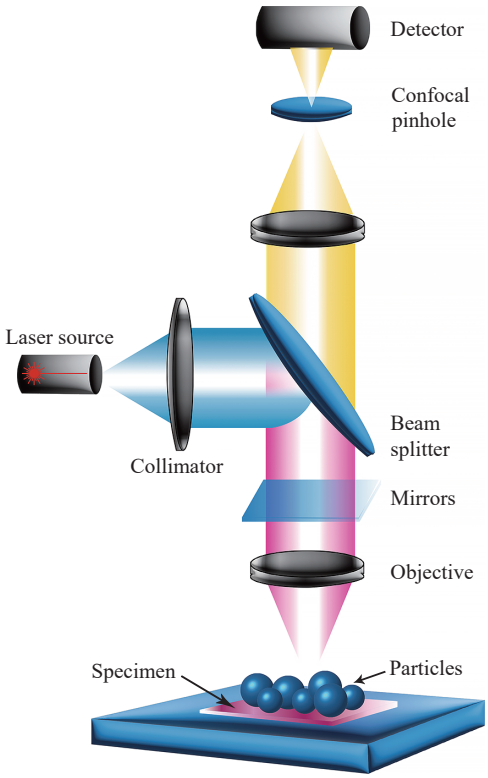

Fig. 15 Schematic of confocal microscopy (CM) including a laser, detector, pinhole, galvanometer mirrors, objective lenses, and beam splitter.

6.2 Refractive index matched scanning (RIMS)

Refractive index matched scanning (RIMS) is a technique used in particle flow field studies to improve the visibility of particles in transparent or translucent media (Dijksman et al., 2013; 2017). It involves the use of a matching fluid or medium with a refractive index similar to that of the particles or surrounding medium. This paper (Dijksman et al., 2012) provides a comprehensive review of the use of RIMS to study densely packed granular materials and suspensions.

Fig. 16 represents a schematic of the RIMS. To initiate RIMS, the first step involves selecting a refractive index matching fluid that aligns with either the refractive index of the particles or that of the surrounding medium. This fluid is usually a transparent liquid, such as a mixture of glycerol and water or silicone oil, with carefully controlled optical properties. When the refractive index of the matching fluid closely matches that of the particles or surrounding medium, it reduces the refractive index mismatch between the particles and the fluid. This minimises the light scattering and refraction at the particle-fluid interface, resulting in improved particle visibility. The experimental setup involves immersing the particles in a refractive index-matching fluid. The fluid fills the gaps between the particles, effectively matching the refractive indices of the particles and the fluid. This allows for clearer observation and imaging of particle positions, trajectories, and interactions (Barés et al., 2020; Dijksman et al., 2010).

RIMS is employed across a range of scientific domains to study particle flows (Barés et al., 2020) and suspensions (Ojeda-Mendoza et al., 2018). RIMS also finds applications in multiphase flows (Poelma, 2020), biological systems (Khan et al., 2021), chemical engineering processes

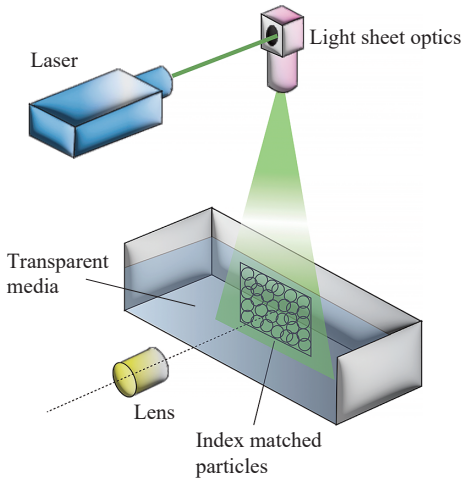

Fig. 16 The setup comprises a laser sheet, a refractive index matching fluid, and particles with matched refractive indices.

(Häfeli et al., 2016), geological and environmental studies (Sather et al., 2023), material characterisation (Butscher et al., 2012), and fluidised beds (Reddy et al., 2013).

6.3 Magnetic resonance imaging (MRI)

Over the past few decades, various types of MRI systems have emerged, ranging from compact benchtop setups to large (pre-)clinical scanners. All these systems have basic components in common, including a magnet providing a magnetic field, gradient coils, and radiofrequency (RF) transmit and receive coils. A detailed explanation of the different types of MRI scanners is well described in a recent review article (Clarke et al., 2023). MRI relies on nuclear magnetic resonance (NMR) principles. When a material, like water with NMR-active hydrogens encounters a strong magnetic field, its nuclear spins will align. Transmit coils send RF pulses, causing nuclear spins to briefly absorb and emit energy. Gradient coils create spatial field variations for precise signal localisation. By manipulating gradients and RF pulses, MRI systems can create detailed images based on nuclear spin properties like density and relaxation times (Dale et al., 2015). In MRI imaging, two crucial parameters are relaxation times, known as T_1 (spin–lattice relaxation time) and T_2 (spin–spin relaxation time). T_1 and T_2 relaxation times determine how quickly the nuclear spins return to equilibrium or lose phase coherence. These times depend on various factors, including the material type being imaged and the properties of the MRI system itself. These factors are essential for creating contrast in images and providing information about material characteristics. Meanwhile, receive coils capture the emitted RF signals, which are then processed to produce the final images, providing invaluable insights into the structure and composition of materials without ionising radiation. MRI can also measure displacements over time, and thus quantify both self-diffusion behaviour as well as net displacements. The latter is the basis of the velocimetric assessment of flow, which can provide insights into the non-Newtonian behaviour of complex fluids.

While MRI is primarily known for its medical applications, it can also be adapted for material studies, including granular systems (Stannarius, 2017). **Fig. 17** shows a schematic of a (pre-)clinical MRI setup used for particle flow measurements. In the context of particle flow fields, MRI can provide insights into the internal structure, porosity, and flow patterns of granular materials. It can track the motion and distribution of fluids or particles within the system (Wang et al., 2022a). Using suitable contrast agents, one can differentiate between different phases or components within the granular system, enabling the visualisation and quantification of particle flows.

6.4 X-ray imaging

X-ray imaging is a valuable technique for studying particle flow fields in granular materials (Chen et al., 2021). **Fig. 18** depicts a schematic of X-ray imaging. It utilises X-rays, which are a form of electromagnetic radiation, to penetrate the material and generate images that reveal the internal structure, particle arrangements, and flow behaviour. X-rays have high energy and short wavelengths, allowing them to penetrate solid or dense materials, including most non-metallic granular systems. As X-rays pass through the material, they interact with the particles and undergo attenuation, which means that their intensity decreases based on the density and composition of the material (Hermanek et al., 2018).

6.4.1 Radiographic imaging

In X-ray radiography, a beam of X-rays is directed towards the material, and a detector captures the X-rays that pass through. The detected X-rays are converted into an image representing the attenuation of the X-rays within the material. This image provides information about the distribution of particles, their packing density, and the presence

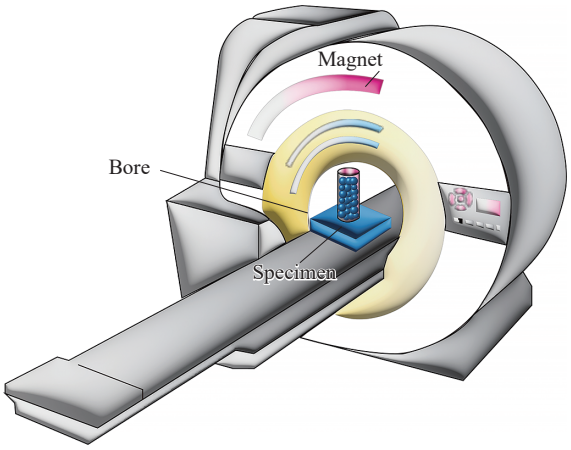

Fig. 17 Schematic of a (pre-)clinical MRI machine. This allows for the placement of a container filled with particles on the specimen, enabling the imaging of static particle arrangements.

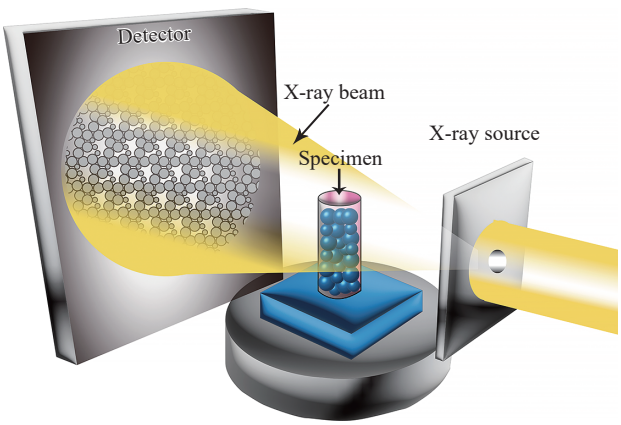

Fig. 18 Schematic of the X-ray imaging setup. The setup consists of an X-ray source, a detector, and a specimen or rotating table where you place a container filled with particles.

of voids or channels within the granular system (Guillard et al., 2017).

6.4.2 X-ray computed tomography (CT)

CT is a more advanced technique that combines multiple X-ray radiographic images taken from different angles to reconstruct a detailed three-dimensional image of the material (Withers et al., 2021). By capturing X-ray projections at various angles, CT can provide volumetric information, enabling the visualisation of particle flow patterns and internal structures in greater detail (Lyu et al., 2023; Mohsin Thakur et al., 2020).

6.4.3 Ultrafast electron beam X-ray computed tomography

Ultrafast electron beam X-ray computed tomography (CT) is an advanced imaging technique that combines ultrafast electron beams and CT. It aims to provide high-speed, high-resolution imaging of dynamic processes, such as multiphase flow in vertical pipes (Fischer and Hampel, 2010), in a gas-solid fluidised bed, dynamic quality control of agricultural products, particle flow fields, and within granular materials (Bieberle et al., 2012).

Fig. 19 shows a schematic of the high-performance ROFEX (ROssendorf Fast Electron beam X-ray tomography) imaging method, designed for non-invasive exploration of dynamic processes. This technique boasts an impressive capability of capturing up to 8,000 cross-sectional images per second, providing a spatial resolution of approximately 1 mm. ROFEX employs an ultrafast electron beam as the imaging source. This beam is generated using an electron gun and accelerated to high energies. The electrons act as a source of X-rays through a process called "braking radiation", in which the electron beam interacts with a target material and produces X-ray photons. When an ultrafast electron beam strikes a target material, such as a metal, it produces a broad spectrum of X-ray photons due to the deceleration of the electrons. The X-ray spectrum contains a range of energies that can be tuned and selected depending on the desired imaging characteristics (Frust et al., 2017).

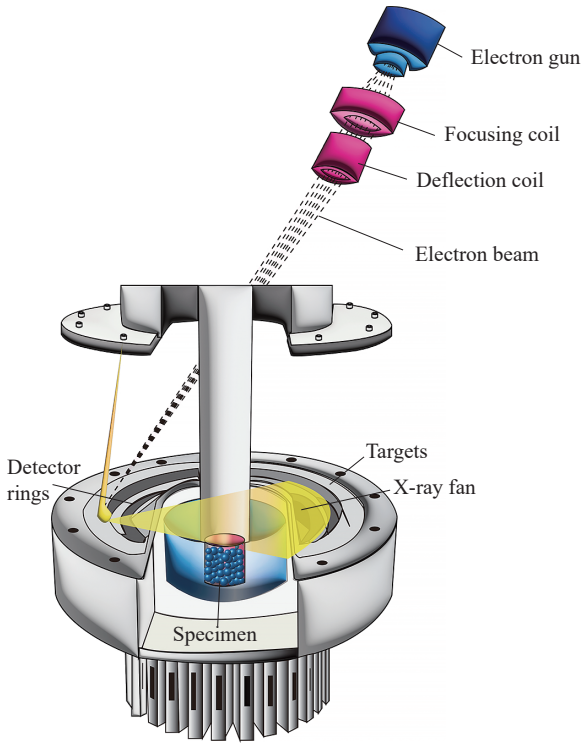

Fig. 19 Schematic of the high-performance ROFEX (ROssendorf Fast Electron beam X-ray tomography) imaging method at Helmholtz-Zentrum Dresden-Rossendorf. ROFEX consists of an electron beam that is generated using an electron gun, focussing coil, deflection coil, X-ray fan, detector rings, and a specimen.

The usefulness of ROFEX in the field of granular materials lies in its ability to provide time-resolved imaging of dynamic processes (Stannarius et al., 2019a). ROFEX can capture fast flow phenomena, particle interactions, and granular rearrangements on a timescale that may not be achievable with other imaging techniques. The reconstructed three-dimensional images obtained through ROFEX can be analysed quantitatively to extract important parameters, such as particle velocities, trajectories, packing densities, and flow rates. Moreover, ROFEX can study multiphase systems (Bieberle and Hampel, 2015), where different components or phases have distinct X-ray attenuation properties.

6.5 Comparative analysis

Table 3 summarises the applicability ranges of various imaging techniques for capturing particle properties. In addition, we compared the advantages, limitations, and

Table 3 Summary of the imaging techniques' applicability ranges for capturing particle properties.

Technique	Particle size	Particle type	Spatial resolution
MRI	µm	Solid particles, liquid droplets, and soft materials	10–100 µm
XRT	sub-µm to mm	Dense- and low-density particles	sub-µm to µm
CM	sub-µm to µm	Fluorescent or highly scattering particles	500 nm to µm
OM	sub-µm to mm	Biological particles, colloids, and solid particles	sub-µm to µm
RIMS	µm to mm	Transparent or translucent particles and fluids	sub-µm to µm

Table 4 Summary and comparison of the advantages, limitations, and typical applications of various particle imaging techniques reviewed in this paper.

Technique	Advantages	Limitations	Typical applications
OM	Versatility and accessibility; morphological properties; real-time observation.	Limited depth of field; particle behaviour analysis; particle tracking limitations; limited to visible light spectrum; size and resolution limitations [a].	Particle behaviour analysis; flow field visualisation; particle size and shape determination.
CM	High spatial resolution 3D imaging; optical sectioning [b]. Rejects out-of-focus light; suitable for transparent samples.	Limited imaging depth; slow imaging speed; limited to relatively thin samples; limited field of view.	Thick or densely packed granular samples; nondynamic particle flow fields; small-scale or microscopic particle flow fields.
RIMS	Enhanced particle visibility; reduced optical distortions; increased imaging depth.	Selection of matching fluid; refractive index sensitivity; experimental constraints [c].	Particle tracking in transparent or translucent media; optically complex or dense systems; void and channel analysis.
MRI	Non-invasive; 3D; multi-phase imaging [d].	Time-consuming and costly; trade-off between spatial and temporal resolution to be set by experts; signal loss and artifacts [e].	Multi-phase interactions; internal flow patterns.
XRT	Non-destructive; high penetration depth; quantitative analysis [f]; high spatial resolution.	Radiation safety; contrast and sensitivity [g]; limited temporal resolution [h]; costly.	Particle distribution in granular materials; internal structure analysis; multi-phase systems.

[a] OM has limitations in resolving particles below the diffraction limit of light.
[b] The ability to selectively focus on a specific plane within the sample enables optical sectioning.
[c] It may introduce additional complexities, such as changes in particle behaviour due to interactions with the matching fluid.
[d] MRI can differentiate between different phases within the granular material, such as solid particles and fluid phases.
[e] Granular materials, especially those with high density or metallic components, can cause signal loss and susceptibility artefacts in MRI images.
[f] XRT can provide quantitative information on particle distributions, void fractions, and packing densities within granular materials.
[g] XRT may face challenges in differentiating materials with similar X-ray attenuation coefficients. Contrast agents can be used to enhance sensitivity.
[h] Slower acquisition times.

typical applications of the various particle imaging techniques reviewed in this paper in **Table 4**.

7. Challenges in imaging of granular flows

Combining imaging with flow testing is pursued to gain a deeper understanding of material behaviour and fluid dynamics. It enables the visualisation of individual particle dynamics (Aliseda and Heindel, 2021), microscale phenomena (Milatz et al., 2021), and complex interactions within materials (L. Li and Iskander, 2022), providing insights that traditional flow testing alone cannot offer. This integration is valuable for validating models (Larsson et al., 2021), optimising industrial processes, characterising materials, and studying fluid dynamics in biological (Moosavi et al., 2014) and geotechnical contexts (Dai et al., 2023). By bridging the macroscopic and microscopic domains, we can enhance our ability to analyse and manipulate materials and fluids, facilitating advancements in various fields and applications. While combining flow tests with particle imaging techniques has opened new frontiers in the study of granular flows, several challenges still persist, presenting opportunities for further research and innovation. In this section, we discuss some current challenges faced in the imaging of granular flows.

7.1 Real-time analysis

Real-time analysis of imaging data is crucial for gaining immediate insights into granular flow behaviours. However, processing large datasets generated during experiments can be computationally intensive and time-consuming. Streamlining and automating real-time data analysis (Munir et al., 2018) to provide researchers with actionable information during experiments is an ongoing challenge.

One can observe and interpret data as it is generated, allowing them to make adjustments to the experiment in real time. This immediate feedback is valuable for optimising experimental conditions, making critical decisions, and ensuring data quality. Real-time analysis enables the identification of key events or phenomena as they occur within the granular flow. It allows for quality control by promptly identifying issues with data acquisition or imaging

equipment. One can address problems such as sensor malfunctions or calibration errors in real time.

7.2 Particle tracking in complex flows

Accurate tracking of individual particles within complex flow fields is essential for understanding granular flow dynamics. However, in real-world scenarios, particles can experience a wide range of interactions, including collision, adhesion, and fragmentation. Developing robust tracking algorithms capable of handling such complexities and uncertainties is an ongoing research challenge (Liang et al., 2021).

Accurately tracking the motion of individual particles involves monitoring the trajectories, velocities, and interactions of particles as they move within the flow. This tracking provides critical data for characterising flow behaviour, identifying flow regimes, and studying phenomena like particle collisions and adhesion.

Various methods and techniques can be employed to address the challenges of particle tracking in granular flows (Mallery et al., 2020; Wang et al., 2019). Particle Tracking Velocimetry (PTV) methods involve tracking individual particles in successive frames of imaging data to calculate particle trajectories and velocities (Mäkiharju et al., 2022). This approach can capture complex particle interactions and flow dynamics. Particle Image Velocimetry (PIV) techniques use the displacement of particle patterns in successive images to calculate flow velocities. Although not particle-specific, PIV is valuable for analysing bulk flow behaviour (Molina et al., 2021; Sarno et al., 2019). Advanced algorithms, often based on machine learning, are employed to automate and improve particle tracking accuracy, especially in complex and noisy flows (Duarte and Vlimant, 2022).

7.3 Integration of multimodal imaging

Combining multiple imaging modalities, such as Neutron and X-ray imaging (Sleiman et al., 2021; Vego et al., 2023b), offers the potential for richer data. However, the seamless integration of these techniques to provide complementary information poses technical challenges. Ensuring compatibility and synchronisation between different imaging systems is an area that requires further attention. While the integration of flow tests with particle imaging techniques has propelled our understanding of granular flows, addressing these current challenges will be crucial for pushing the boundaries of knowledge in this field.

8. Recent advances in coupling flow testing and particle imaging in granular flows

In recent years, significant strides have been made in the field of granular and particulate systems through the integration of dynamic flow measurements with particle imaging techniques.

8.1 X-ray rheography

In this context, Baker et al. (2018) introduced a novel X-ray rheography technique (**Fig. 20**) for studying the flow of granular materials, addressing the limitations of traditional methods that require model materials or intermittent motion stoppage. The authors used correlation analysis of high-speed X-ray radiographs from three directions to directly reconstruct three-dimensional velocities, enabling the study of continuous granular flows. Surprisingly, in a steady granular system, they discovered a compressible flow field with planar streamlines, despite the presence of non-planar confining boundaries. This finding contrasts with the behaviour of Newtonian fluids. The paper also discusses the impact of particle shape on flow and suggests future applications of the technique in the study of various soft matter systems, including biological tissues, geomaterials, and foams.

8.2 Multiple imaging methods

The integration of multiple imaging methods has enabled multiscale analysis, allowing researchers to gain insights into particle behaviour that spans the microscale to the macroscale (**Fig. 21**) (Vego et al., 2023a). This approach has proven particularly beneficial when studying complex and heterogeneous particle systems, such as those found in food products.

8.3 Rheo-MRI

In addition to the recent advances in the use of X-ray tomography techniques, the combination of rheology and

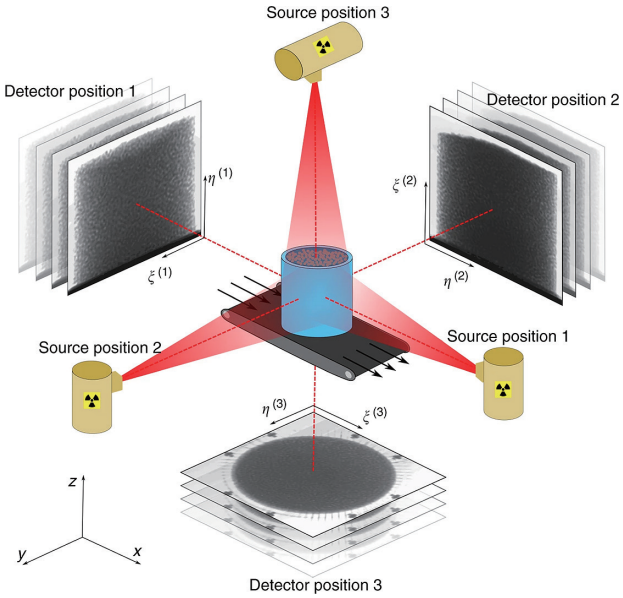

Fig. 20 Experimental configuration for rheography. The particles within the blue cylinder are subject to shearing from below. The diagram highlights the three X-ray source locations in yellow. Reprinted from Ref. (Baker et al., 2018) under the terms of the CC-BY 4.0 license. Copyright: (2018) The Authors, published by Springer Nature.

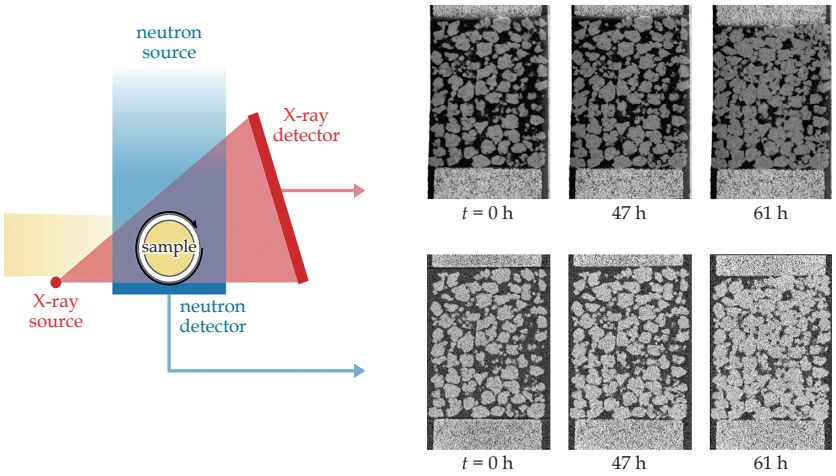

Fig. 21 Neutron and X-ray tomographic scans. The **top row** displays vertical sections from X-ray tomography, whereas the **bottom row** shows equivalent slices from neutron tomography. Reprinted from Ref. (Vego et al., 2023b) under the terms of the CC-BY 4.0 license. Copyright: (2023) The Authors, published by Springer Nature.

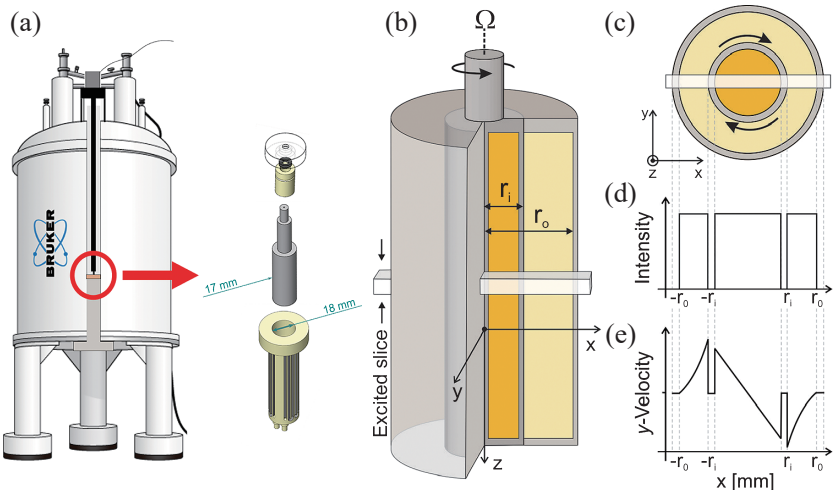

Fig. 22 **(a)** Schematic of a Rheo-MRI setup, **(b)** experimental Couette cell geometry, **(c)** top-down view of the cell, **(d)** one-dimensional concentration and **(e)** *y*-velocity within the excited slice. This figure is taken with permission from Refs. (Milc et al., 2022; Serial et al., 2019).

MRI is a powerful technique used in various systems to study the mechanical properties and flow behaviour of complex fluids and soft materials (Serial et al., 2021; 2022). A rheo-cell, typically with a Couette or Cone-Plate geometry, is placed in an MRI system, allowing velocimetric measurements. By combining this with *in situ* or *ex situ* measurement of torque, local rheological properties such as viscosity, shear stress, and shear rate can be measured (**Fig. 22**). This combination provides insights into the relationship between the material's rheological response and its microstructure during flow (Coussot, 2020; Milc et al., 2022). Rheo-MRI is typically used in velocimetric mode, meanwhile relaxometric behaviour can give insights in structure formation/degradation. Maps of material density can provide insights into shear-induced migration.

9. Critical review and future directions

The integration of flow tests with particle imaging techniques has undeniably advanced our understanding of granular materials and complex fluids. These combined approaches have enabled researchers to uncover critical information about particle behaviour and interactions at the microscale, offering insights that were previously elusive. Shear testers such as the Schulze shear tester and FT4 powder flow tester have provided valuable data on bulk flow properties, while imaging techniques such as MRI, X-ray imaging, and confocal microscopy have facilitated the visualisation of particle dynamics. However, challenges persist, particularly in the integration of flow tests with imaging, which often involves complex experimental set-ups and resource-intensive data processing.

To overcome these challenges, it is natural to suggest the development of more simple, small-scale flow testers designed to align with selected 3D imaging techniques, specifically tailored to the material being investigated. A straightforward flow tester can take the form of a basic tube

or container equipped with motors and sensors for flow analysis. In addition, maintaining a database containing information about the studied material, flow geometry, and raw images could prove highly beneficial and time-saving for researchers seeking to replicate similar studies. Another crucial ongoing improvement involves integrating advanced processing techniques and conducting real-time flow analysis. This enhancement can significantly increase the efficiency of the testing procedure, while also addressing the cost considerations associated with 3D imaging facilities.

The future of this integration holds promise in the development of high-speed, high-resolution imaging methods, such as X-ray rheography and high-speed X-ray imaging (such as ROFEX), providing detailed insights into dynamic processes within granular materials. Artificial intelligence further contributes by enabling real-time image analysis to manage the overwhelming volume of data generated. Moreover, the integration of computational simulations, such as Discrete Element Method (DEM) or Molecular Dynamic (MD) simulations, with experimental flow tests and imaging offers a comprehensive understanding of complex systems, allowing validation and calibration of theoretical models against empirical observations.

10. Conclusion

We explored mechanical testers and particle imaging techniques and highlighted their combined potential. By merging these fields, we can gain unparalleled insights into the dynamics of granular materials and complex fluids, deepening our understanding of bulk flow behaviours. We have explored various shear testers, from the Schulze shear tester to the FT4 powder flow tester, each of which provides valuable insights into the macroscopic properties of materials under shear. Simultaneously, refractive index matching, MRI, and X-ray imaging have emerged as powerful tools for capturing microscale particle interactions and flow patterns. We also highlighted the need for technological advancements in imaging methods, especially ultrafast imaging and advanced data analysis techniques, to meet the growing demands for particle-level analysis.

Acknowledgments

This project received funding from the European Union's Horizon 2020 research and innovation program under the Marie Skłodowska-Curie grant agreement No 812638. We acknowledge the valuable discussions with Cino Viggiani, Ralf Stannarius, and Frans Leermakers.

Nomenclature

CP	Cone–plate geometry
DC	Double-cone geometry
DEM	Discrete Element Method
FEM	Finite Element Modelling
PIV	Particle Image Velocimetry
PP	Plate–plate geometry
PTV	Particle Tracking Velocimetry
RF	Radio frequent
RST-M	Ring Shear Tester with size medium
RST-XS	Ring Shear Tester with size x-small
T_1	Spin–lattice relaxation time (s)
T_2	Spin–spin relaxation time (s)
ff_c	Flowability index (-)
F	Force (N)
H	Thickness of the particle layer (mm)
r_i	Radius of the inner cylinder (mm)
r_o	Radius of the outer cylinder (mm)
R_s	Radius of the inner cylinder or split radius in the split-bottom shear cell (mm)
R_o	Radius of the outer cylinder in the split-bottom shear cell (mm)
τ	Shear stress (Pa)
τ_{sh}	Shear stress at the shear point (Pa)
τ_{pre}	Shear stress at pre-shear (Pa)
$\sigma_{1,2}$	Consolidation stress (Pa)
σ_c	Compressive strength or unconfined yield strength (Pa)
ω	Rotation speed or angular velocity (rpm)
θ	Dynamic angle of repose (-)
ϕ	Angle of internal friction (-)
ρ_b or ρ_{bulk}	Bulk density (kg·m^{-3})
ρ_{Tapped}	Tapped density (kg·m^{-3})

References

Aigner A., Schneiderbauer S., Kloss C., Pirker S., Determining the coefficient of friction by shear tester simulation, PARTICLES III: Proceedings of the III International Conference on Particle-Based Methods: Fundamentals and Applications, (2013) 335–342. <http://hdl.handle.net/2117/188464> accessed 24052024.

Akers R.J., The certification of a limestone powder for Jenike shear testing, EUR14022, (1992).

Aliseda A., Heindel T.J., X-ray flow visualization in multiphase flows, Annual Review of Fluid Mechanics, 53 (2021) 543–567. https://doi.org/10.1146/annurev-fluid-010719-060201

Amon A., Born P., Daniels K.E., Dijksman J.A., Huang K., Parker D., Schröter M., Stannarius R., Wierschem A., Preface: focus on imaging methods in granular physics, Review of Scientific Instruments, 88(5) (2017) 051701. https://doi.org/10.1063/1.4983052

Baker J., Guillard F., Marks B., Einav I., X-ray rheography uncovers planar granular flows despite non-planar walls, Nature Communications, 9(1) (2018) 5119. https://doi.org/10.1038/s41467-018-07628-6

Balla A., Stress conditions in triaxial compression, Journal of the Soil Mechanics and Foundations Division, 86(6) (1960) 57–84. https://doi.org/10.1061/JSFEAQ.0000312

Barés J., Brodu N., Zheng H., Dijksman J.A., Transparent experiments: releasing data from mechanical tests on three dimensional hydrogel sphere packings, Granular Matter, 22 (2020) 1–7. https://doi.org/10.1007/s10035-019-0985-4

Bastiaansen T.M.M., Benders R.T., de Vries S., Hendriks W.H., Thomas M., Bosch G., Dijksman J.A., Capillary rheometry as a model methodology for obtaining insight in feed mash behaviour at conditions approximating pellet manufacturing, Animal Feed Science and Technology, 303 (2023) 115693. https://doi.org/10.1016/j.anifeedsci.2023.115693

Beaulieu C., Vidal D., Niyonkuru C., Wachs A., Chaouki J., Bertrand F., Effect of particle angularity on flow regime transitions and segregation of bidisperse blends in a rotating drum, Computational Particle Mechanics, 9 (2022) 443–463. https://doi.org/10.1007/s40571-021-00421-1

Benyaya M., Bolzinger M.-A., Chevalier Y., Ensenat S., Bordes C.,

Pickering emulsions stabilized with differently charged particles, Soft Matter, 19(25) (2023) 4780–4793. https://doi.org/10.1039/D3SM00305A

Berry R.J., Bradley M.S.A., Development of the Brookfield powder flow tester. Proceedings of the School of Engineering, Wolfson Centre for Bulk Solids Handling Technology, 2010. <http://gala.gre.ac.uk/id/eprint/7163> accessed 24052024.

Berry R.J., Bradley M.S.A., McGregor R.G., Brookfield powder flow tester–Results of round robin tests with CRM-116 limestone powder, Proceedings of the Institution of Mechanical Engineers, Part E: Journal of Process Mechanical Engineering, 229(3) (2015) 215–230. https://doi.org/10.1177/0954408914525387

Bieberle M., Barthel F., Hoppe D., Banowski M., Wagner M., Lucas D., Stürzel T., Hampel U., Ultrafast electron beam X-ray computed tomography for 2D and 3D two-phase flow imaging, 2012 IEEE International Conference on Imaging Systems and Techniques Proceedings, (2012) 605–610. https://doi.org/10.1109/IST.2012.6295548

Bieberle M., Hampel U., Level-set reconstruction algorithm for ultrafast limited-angle X-ray computed tomography of two-phase flows, Philosophical Transactions of the Royal Society A: Mathematical, Physical and Engineering Sciences, 373(2043) (2015) 20140395. https://doi.org/10.1098/rsta.2014.0395

Bilgili E., Yepes J., Stephenson L., Johanson K., Scarlett B., Stress inhomogeneity in powder specimens tested in the Jenike shear cell: myth or fact?, Particle & Particle Systems Characterization, 21(4) (2004) 293–302. https://doi.org/10.1002/ppsc.200400942

Boyer F., Guazzelli É., Pouliquen O., Unifying suspension and granular rheology, Physical Review Letters, 107(18) (2011) 188301. https://doi.org/10.1103/PhysRevLett.107.188301

Butscher D., Hutter C., Kuhn S., von Rohr P., Particle image velocimetry in a foam-like porous structure using refractive index matching: a method to characterize the hydrodynamic performance of porous structures, Experiments in Fluids, 53 (2012) 1123–1132. https://doi.org/10.1007/s00348-012-1346-9

Cataldo A., Vallone M., Tarricone L., Cannazza G., Cipressa M., TDR moisture estimation for granular materials: an application in agro-food industrial monitoring, IEEE Transactions on Instrumentation and Measurement, 58(8) (2009) 2597–2605. https://doi.org/10.1109/TIM.2009.2015636

Cavarretta I., O'Sullivan C., The mechanics of rigid irregular particles subject to uniaxial compression, Géotechnique, 62(8) (2012) 681–692. https://doi.org/10.1680/geot.10.P.102

Chen P., Ottino J.M., Lueptow R.M., Onset mechanism for granular axial band formation in rotating tumblers, Physical Review Letters, 104(18) (2010) 188002. https://doi.org/10.1103/PhysRevLett.104.188002

Chen Y., Ma G., Zhou W., Wei D., Zhao Q., Zou Y., Grasselli G., An enhanced tool for probing the microscopic behavior of granular materials based on X-ray micro-CT and FDEM, Computers and Geotechnics, 132 (2021) 103974. https://doi.org/10.1016/j.compgeo.2020.103974

Cheng Z., Wang J., Estimation of contact forces of granular materials under uniaxial compression based on a machine learning model, Granular Matter, 24 (2022) 1–14. https://doi.org/10.1007/s10035-021-01160-z

Clarke D., Hogendoorn W., Penn A., Serial R., Magnetic resonance imaging in granular flows: an overview of recent advances, Particuology, (2023). https://doi.org/10.1016/j.partic.2023.08.007

Coetzee C.J., Els D.N.J., Calibration of discrete element parameters and the modelling of silo discharge and bucket filling, Computers and Electronics in Agriculture, 65(2) (2009) 198–212. https://doi.org/10.1016/j.compag.2008.10.002

Cordts E., Steckel H., Capabilities and limitations of using powder rheology and permeability to predict dry powder inhaler performance, European Journal of Pharmaceutics and Biopharmaceutics, 82(2) (2012) 417–423. https://doi.org/10.1016/j.ejpb.2012.07.018

Couch M.A., Binding D.M., High pressure capillary rheometry of polymeric fluids, Polymer, 41(16) (2000) 6323–6334. https://doi.org/10.1016/S0032-3861(99)00865-4

Coussot P., Progress in rheology and hydrodynamics allowed by NMR or MRI techniques, Experiments in Fluids, 61 (2020) 1–20. https://doi.org/10.1007/s00348-020-03037-y

Cunez F.D., Patel D., Glade R., How particle shape affects granular segregation in industrial and geophysical flows, Proceedings of the National Academy of Sciences, 121 (6) (2023) e2307061121. https://doi.org/10.1073/pnas.2307061121

Curran D.R., Seaman L., Cooper T., Shockey D.A., Micromechanical model for comminution and granular flow of brittle material under high strain rate application to penetration of ceramic targets, International Journal of Impact Engineering, 13(1) (1993) 53–83. https://doi.org/10.1016/0734-743X(93)90108-J

Dai X., He L., Wu W., Chen J., Visualization experiment technology based on transparent geotechnical materials and its engineering application, Journal of Visualization, 26(1) (2023) 145–159. https://doi.org/10.1007/s12650-022-00863-6

Dale B.M., Brown M.A., Semelka R.C., MRI: Basic Principles and Applications, John Wiley & Sons, 2015, ISBN: 9781119013051. https://doi.org/10.1002/9781119013068

Deng T., Garg V., Diaz L.P., Markl D., Brown C., Florence A., Bradley M.S.A., Comparative studies of powder flow predictions using milligrams of powder for identifying powder flow issues, International Journal of Pharmaceutics, 628 (2022) 122309. https://doi.org/10.1016/j.ijpharm.2022.122309

Dijksman J.A., Brodu N., Behringer R.P., Refractive index matched scanning and detection of soft particles, Review of Scientific Instruments, 88(5) (2017) 51807. https://doi.org/10.1063/1.4983047

Dijksman J.A., Rietz F., Lőrincz K.A., Van Hecke M., Losert W., Invited article: refractive index matched scanning of dense granular materials, Review of Scientific Instruments, 83(1) (2012) 011301. https://doi.org/10.1063/1.3674173

Dijksman J.A., van Hecke M., Granular flows in split-bottom geometries, Soft Matter, 6 (2010) 2901–2907. https://doi.org/10.1039/B925110C

Dijksman J.A., Wandersman E., Slotterback S., Berardi C.R., Updegraff W.D., van Hecke M., Losert W., From frictional to viscous behavior: three-dimensional imaging and rheology of gravitational suspensions, Physical Review E, 82(6) (2010) 60301. https://doi.org/10.1103/PhysRevE.82.060301

Dijksman J.A., Zheng H., Behringer R.P., Imaging soft sphere packings in a novel triaxial shear setup, AIP Conference Proceedings, 1542 (2013) 457–460. https://doi.org/10.1063/1.4811966

Divya S., Ganesh G.N.K., Characterization of powder flowability using FT4–powder rheometer, Journal of Pharmaceutical Sciences and Research, 11(1) (2019) 25–29. <https://www.jpsr.pharmainfo.in/Documents/Volumes/vol11Issue01/jpsr11011906.pdf> accessed 11062024.

Du H., Lu H., Tang J., Liu H., Characterization of powder flow properties from micron to nanoscale using FT4 powder rheometer and PT-X powder tester, Particuology, 75 (2023) 1–10. https://doi.org/10.1016/j.partic.2022.05.014

Duarte J., Vlimant J.-R., Graph neural networks for particle tracking and reconstruction, in: Calafiura P., Rousseau D., Terao K. (Eds.), Artificial Intelligence for High Energy Physics, 2022, pp. 387–436, ISBN: 9789811234026. https://doi.org/10.1142/9789811234033_0012

Duran J., Sands, Powders, and Grains: An Introduction to the Physics of Granular Materials, Springer Science & Business Media, 2012, ISBN: 9780387986562. https://doi.org/10.1007/978-1-4612-0499-2

Faug T., Impact force of granular flows on walls normal to the bottom: slow versus fast impact dynamics, Canadian Geotechnical Journal, 58(1) (2020) 114–124. https://doi.org/10.1139/cgj-2019-0399

Fenistein D., van Hecke M., Wide shear zones in granular bulk flow, Nature, 425 (2003) 256. https://doi.org/10.1038/425256a

Fenistein D., van de Meent J.-W., van Hecke M., Universal and wide shear zones in granular bulk flow, Physical Review Letters, 92 (2004) 94301. https://doi.org/10.1103/PhysRevLett.92.094301

Fiedor S.J., Ottino J.M., Dynamics of axial segregation and coarsening of dry granular materials and slurries in circular and square tubes, Physical Review Letters, 91(24) (2003) 244301. https://doi.org/10.1103/PhysRevLett.91.244301

Fischer F., Hampel U., Ultra-fast electron beam X-ray computed tomography for two-phase flow measurement, Nuclear Engineering and

Design, 240(9) (2010) 2254–2259. https://doi.org/10.1016/j.nucengdes.2009.11.016
Francia V., Yahia L.A.A., Ocone R., Ozel A., From quasi-static to intermediate regimes in shear cell devices: theory and characterisation, KONA Powder and Particle Journal, 38 (2021) 3–25. https://doi.org/10.14356/kona.2021018
Freeman R., The importance of air content on the rheology of powders: an empirical study, American Laboratory, 36(23) (2004) 8–10.
Freeman R., Measuring the flow properties of consolidated, conditioned and aerated powders—a comparative study using a powder rheometer and a rotational shear cell, Powder Technology, 174(1–2) (2007) 25–33. https://doi.org/10.1016/j.powtec.2006.10.016
Frust T., Wagner M., Stephan J., Juckeland G., Bieberle A., Rapid data processing for ultrafast X-ray computed tomography using scalable and modular CUDA based pipelines, Computer Physics Communications, 219 (2017) 353–360. https://doi.org/10.1016/j.cpc.2017.05.025
Gaitonde A.J.U., Thermal transport in lithium ion batteries: an experimental investigation of interfaces and granular materials, Master's thesis, Purdue University, (2016). https://docs.lib.purdue.edu/open_access_theses/850
Gillemot K.A., Somfai E., Börzsönyi T., Shear-driven segregation of dry granular materials with different friction coefficients, Soft Matter, 13(2) (2017) 415–420. https://doi.org/10.1039/C6SM01946C
Graziano R., Preziosi V., Uva D., Tomaiuolo G., Mohebbi B., Claussen J., Guido S., The microstructure of Carbopol in water under static and flow conditions and its effect on the yield stress, Journal of Colloid and Interface Science, 582 (2021) 1067–1074. https://doi.org/10.1016/j.jcis.2020.09.003
Grima A., Mills B.P., Wypych P.W., Investigation of measuring wall friction on a large scale wall friction tester and the Jenike direct shear tester, University of Wollongong Research Online, (2010). https://ro.uow.edu.au/engpapers/2671
Guillard F., Marks B., Einav I., Dynamic X-ray radiography reveals particle size and shape orientation fields during granular flow, Scientific Reports, 7(1) (2017) 8155. https://doi.org/10.1038/s41598-017-08573-y
Guo C., Ye K., Xu Y., Dai X., Zheng J., Ya M., Discharge characteristics of conical and hyperbolic hoppers based on discharge time distribution, Powder Technology, 426 (2023) 118665. https://doi.org/10.1016/j.powtec.2023.118665
Guo Y., Buettner K., Lane V., Wassgren C., Ketterhagen W., Hancock B., Curtis J., Computational and experimental studies of flexible fiber flows in a normal-stress-fixed shear cell, AIChE Journal, 65(1) (2019) 64–74. https://doi.org/10.1002/aic.16397
Häfeli R., Rüegg O., Altheimer M., von Rohr P.R., Investigation of emulsification in static mixers by optical measurement techniques using refractive index matching, Chemical Engineering Science, 143 (2016) 86–98. https://doi.org/10.1016/j.ces.2015.12.022
Han T., Comparison of wall friction measurements by Jenike shear tester and ring shear tester, KONA Powder and Particle Journal, 29 (2011) 118–124. https://doi.org/10.14356/kona.2011014
Hare C., Ghadiri M., Stress and strain rate analysis of the FT4 powder rheometer, EPJ Web of Conferences, 140 (2017) 3034. https://doi.org/10.1051/epjconf/201714003034
Hare C., Zafar U., Ghadiri M., Freeman T., Clayton J., Murtagh M.J., Analysis of the dynamics of the FT4 powder rheometer, Powder Technology, 285 (2015) 123–127. https://doi.org/10.1016/j.powtec.2015.04.039
Hare C., Zafar U., Ghadiri M., Freeman T., Clayton J., Murtagh M.J.. Correction to "Analysis of the dynamics of the FT4 powder rheometer" [Powder Technol. 285 (2015) 123–127], Powder Technology, 315 (2017) 37–38. https://doi.org/10.1016/j.powtec.2017.02.061
He S., Wang Y., Zhou Z., Gan J., Yu A., Pinson D., Size-induced axial segregation of ellipsoids in a rotating drum, Powder Technology, 422 (2023) 118490. https://doi.org/10.1016/j.powtec.2023.118490
Henann D.L., Kamrin K., A predictive, size-dependent continuum model for dense granular flows, Proceedings of the National Academy of Sciences, 110(17) (2013) 6730–6735. https://doi.org/10.1073/pnas.1219153110
Hermanek P., Rathore J.S., Aloisi V., Carmignato S., Principles of X-ray computed tomography, Industrial X-Ray Computed Tomography, (2018) 25–67. https://doi.org/10.1007/978-3-319-59573-3_2
Hooiveld E., van der Kooij H.M., Kisters M., Kodger T.E., Sprakel J., van der Gucht J., In-situ and quantitative imaging of evaporation-induced stratification in binary suspensions, Journal of Colloid and Interface Science, 630 (2023) 666–675. https://doi.org/10.1016/j.jcis.2022.10.103
Huang P., Miao Q., Ding Y., Sang G., Jia M., Research on surface segregation and overall segregation of particles in a rotating drum based on stacked image, Powder Technology, 382 (2021) 162–172. https://doi.org/10.1016/j.powtec.2020.12.063
Inagaki S., Yoshikawa K., Traveling wave of segregation in a highly filled rotating drum, Physical Review Letters, 105(11) (2010) 118001. https://doi.org/10.1103/PhysRevLett.105.118001
Jenike A.W., Gravity flow of bulk solids. Bulletin No. 108, Utah Engineering Experiment Station, University of Utah, (1961).
Jenike A.W., Storage and flow of solids. Bulletin No. 123, Utah State University, (1964). <https://digital.library.unt.edu/ark:/67531/metadc1067072/m2/1/high_res_d/5240257.pdf> accessed 24052024.
Juliano P., Barbosa-Cánovas G.V., Food powders flowability characterization: theory, methods, and applications, Annual Review of Food Science and Technology, 1 (2010) 211–239. https://doi.org/10.1146/annurev.food.102308.124155
Khala M.J., Hare C., Wu C.-Y., Venugopal N., Murtagh M.J., Freeman T., Density and size-induced mixing and segregation in the FT4 powder rheometer: an experimental and numerical investigation, Powder Technology, 390 (2021) 126–142. https://doi.org/10.1016/j.powtec.2021.05.027
Khan R., Gul B., Khan S., Nisar H., Ahmad I., Refractive index of biological tissues: review, measurement techniques, and applications, Photodiagnosis and Photodynamic Therapy, 33 (2021) 102192. https://doi.org/10.1016/j.pdpdt.2021.102192
Koynov S., Glasser B., Muzzio F., Comparison of three rotational shear cell testers: powder flowability and bulk density, Powder Technology, 283 (2015) 103–112. https://doi.org/10.1016/j.powtec.2015.04.027
Larsson S., Rodríguez Prieto J.M., Gustafsson G., Häggblad H.-Å., Jonsén P., The particle finite element method for transient granular material flow: modelling and validation, Computational Particle Mechanics, 8 (2021) 135–155. https://doi.org/10.1007/s40571-020-00317-6
Laun H.M., Capillary rheometry for polymer melts revisited, Rheologica Acta, 43 (2004) 509–528. https://doi.org/10.1007/s00397-004-0387-2
Le T.-T., Investigation of force transmission, critical breakage force and relationship between micro-macroscopic behaviors of agricultural granular material in a uniaxial compaction test using discrete element method, Particulate Science and Technology, 40(5) (2022) 620–637. https://doi.org/10.1080/02726351.2021.1983904
Leaper M.C., Measuring the flow functions of pharmaceutical powders using the Brookfield powder flow tester and Freeman FT4, Processes, 9(11) (2021) 2032. https://doi.org/10.3390/pr9112032
Leturia M., Benali M., Lagarde S., Ronga I., Saleh K., Characterization of flow properties of cohesive powders: a comparative study of traditional and new testing methods, Powder Technology, 253 (2014) 406–423. https://doi.org/10.1016/j.powtec.2013.11.045
Li L., Iskander M., Visualization of interstitial pore fluid flow, Journal of Imaging, 8(2) (2022) 32. https://doi.org/10.3390/jimaging8020032
Li R., Xiu W., Liu B., Zheng G., Yang H., Velocity distribution of rice particles in a rotating drum, Powder Technology, 386 (2021) 394–398. https://doi.org/10.1016/j.powtec.2021.03.050
Liang J., Cai S., Xu C., Chen T., Chu J., DeepPTV: particle tracking velocimetry for complex flow motion via deep neural networks, IEEE Transactions on Instrumentation and Measurement, 71 (2021) 1–16. https://doi.org/10.1109/TIM.2021.3120127
Lochab V., Yee A., Yoda M., Conlisk A.T., Prakash S., Dynamics of colloidal particles in microchannels under combined pressure and electric potential gradients, Microfluidics and Nanofluidics, 23 (2019) 1–13. https://doi.org/10.1007/s10404-019-2304-0
Lu K., Brodsky E.E., Kavehpour H.P., Shear-weakening of the transitional

regime for granular flow, Journal of Fluid Mechanics, 587 (2007) 347–372. https://doi.org/10.1017/S0022112007007331
Luding S., The effect of friction on wide shear bands, Particulate Science and Technology, 26(1) (2007) 33–42. https://doi.org/10.1080/02726350701759167
Luo Q., Zheng Q.J., Yu A.B., Finite element investigation of granular dynamics in a split-bottom shear cell, Powder Technology, 314 (2017) 121–128. https://doi.org/10.1016/j.powtec.2016.09.069
Luo S., Weinell C.E., Okkels F., Østergård A.L., Kiil S., On-line, non-Newtonian capillary rheometry for continuous and in-line coatings production, Journal of Coatings Technology and Research, 18 (2021) 611–626. https://doi.org/10.1007/s11998-020-00447-9
Lyu Q., Chen A., Jia J., Singh A., Dai P., Fluids flow in granular aggregate packings reconstructed by high-energy X-ray computed tomography and lattice Boltzmann method, Computers & Fluids, 253 (2023) 105787. https://doi.org/10.1016/j.compfluid.2023.105787
Mackley M.R., Rutgers R.P.G., Capillary rheometry, in: Collyer A.A., Clegg D.W. (Eds.), Rheological Measurement, 1998, pp. 167–189, ISBN: 978-0-412-72030-7. https://doi.org/10.1007/978-94-011-4934-1_5
Mäkiharju S.A., Dewanckele J., Boone M., Wagner C., Griesser A. Tomographic X-ray particle tracking velocimetry: proof-of-concept in a creeping flow, Experiments in Fluids, 63 (2022) 1–12. https://doi.org/10.1007/s00348-021-03362-w
Mallery K., Shao S., Hong J., Dense particle tracking using a learned predictive model, Experiments in Fluids, 61 (2020) 1–14. https://doi.org/10.1007/s00348-020-03061-y
Mani R., Kadau D., Or D., Herrmann H.J., Fluid depletion in shear bands, Physical Review Letters, 109(24) (2012) 248001. https://doi.org/10.1103/PhysRevLett.109.248001
Marchetti L., Hulme-Smith C., Flowability of steel and tool steel powders: a comparison between testing methods, Powder Technology, 384 (2021) 402–413. https://doi.org/10.1016/j.powtec.2021.01.074
Mesri G., Vardhanabhuti B., Compression of granular materials, Canadian Geotechnical Journal, 46(4) (2009) 369–392. https://doi.org/10.1139/T08-123
MiDi G.D.R., On dense granular flows. The European Physical Journal E, 14(4) (2004) 341–365. https://doi.org/10.1140/epje/i2003-10153-0
Milatz M., Hüsener N., Andò E., Viggiani G., Grabe J., Quantitative 3D imaging of partially saturated granular materials under uniaxial compression, Acta Geotechnica, 16(11) (2021) 3573–3600. https://doi.org/10.1007/s11440-021-01315-5
Milc K.W., Serial M.R., Philippi J., Dijksman J.A., van Duynhoven J.P.M., Terenzi C., Validation of temperature-controlled rheo-MRI measurements in a submillimeter-gap Couette geometry, Magnetic Resonance in Chemistry, 60(7) (2022) 606–614. https://doi.org/10.1002/mrc.5157
Mitra H., Pushpadass H.A., Franklin M.E.E., Ambrose R.P.K., Ghoroi C., Battula S.N., Influence of moisture content on the flow properties of basundi mix, Powder Technology, 312 (2017) 133–143. https://doi.org/10.1016/j.powtec.2017.02.039
Mohsin Thakur M., Penumadu D., Bauer C., Capillary suction measurements in granular materials and direct numerical simulations using X-ray computed tomography microstructure, Journal of Geotechnical and Geoenvironmental Engineering, 146(1) (2020) 4019121. https://doi.org/10.1061/(ASCE)GT.1943-5606.0002194
Molina R., Gonzalez V., Benito J., Marsi S., Ramponi G., Petrino R., Implementation of particle image velocimetry for silo discharge and food industry seeds, Applications in Electronics Pervading Industry, Environment and Society, 2021, pp. 3–11, ISBN: 9783030667283. https://doi.org/10.1007/978-3-030-66729-0_1
Moosavi M.-H., Fatouraee N., Katoozian H., Pashaei A., Camara O., Frangi A.F., Numerical simulation of blood flow in the left ventricle and aortic sinus using magnetic resonance imaging and computational fluid dynamics, Computer Methods in Biomechanics and Biomedical Engineering, 17(7) (2014) 740–749. https://doi.org/10.1080/10255842.2012.715638
Moud A.A., Kamkar M., Sanati-Nezhad A., Hejazi S.H., Suspensions and hydrogels of cellulose nanocrystals (CNCs): characterization using microscopy and rheology, Cellulose, 29(7) (2022) 3621–3653. https://doi.org/10.1007/s10570-022-04514-9
Munir M., Baumbach S., Gu Y., Dengel A., Ahmed S., Data analytics: industrial perspective & solutions for streaming data, in: Last M., Bunke H., Kandel A. (Eds.), Data Mining in Time Series and Streaming Databases, World Scientific, 2018, pp. 144–168, ISBN: 9789813228030. https://doi.org/10.1142/9789813228047_0007
Nadimi S., Fonseca J., Andò E., Viggiani G., A micro finite-element model for soil behaviour: experimental evaluation for sand under triaxial compression, Géotechnique, 70(10) (2020) 931–936. https://doi.org/10.1680/jgeot.18.T.030
Nan W., Ghadiri M., Wang Y., Analysis of powder rheometry of FT4: effect of particle shape, Chemical Engineering Science, 173 (2017a) 374–383. https://doi.org/10.1016/j.ces.2017.08.004
Nan W., Gu Y., Stress analysis of blade rheometry by DEM simulations, Powder Technology, 376 (2020) 332–341. https://doi.org/10.1016/j.powtec.2020.08.026
Nan W., Vivacqua V., Ghadiri M., Wang Y., Numerical analysis of air effect on the powder flow dynamics in the FT4 powder rheometer, EPJ Web of Conferences, 140 (2017b) 3036. https://doi.org/10.1051/epjconf/201714003036
Navar R., Leal J.H., Davis B.L., Semelsberger T.A., Rheological effects of moisture content on the anatomical fractions of loblolly pine (Pinus taeda), Powder Technology, 412 (2022) 118031. https://doi.org/10.1016/j.powtec.2022.118031
Nezamabadi S., Radjai F., Mora S., Delenne J.-Y., Ghadiri M. Rheology of soft granular materials: uniaxial compression, EPJ Web of Conferences, 249 (2021) 5008. https://doi.org/10.1051/epjconf/202124905008
Nkurikiye E., Pulivarthi M.K., Bhatt A., Siliveru K., Li Y., Bulk and flow characteristics of pulse flours: a comparative study of yellow pea, lentil, and chickpea flours of varying particle sizes, Journal of Food Engineering, 357 (2023) 111647. https://doi.org/10.1016/j.jfoodeng.2023.111647
Oda M., Deformation mechanism of sand in triaxial compression tests, Soils and Foundations, 12(4) (1972) 45–63. https://doi.org/10.3208/sandf1972.12.4_45
Ogata K., A review: recent progress on evaluation of flowability and floodability of powder, KONA Powder and Particle Journal, 36 (2019) 33–49. https://doi.org/10.14356/kona.2019002
Ojeda-Mendoza G.J., Contreras-Tello H., Rojas-Ochoa L.F., Refractive index matching of large polydisperse silica spheres in aqueous suspensions, Colloids and Surfaces A: Physicochemical and Engineering Aspects, 538 (2018) 320–326. https://doi.org/10.1016/j.colsurfa.2017.10.088
Orband J.L.R., Geldart D., Direct measurement of powder cohesion using a torsional device, Powder Technology, 92(1) (1997) 25–33. https://doi.org/10.1016/S0032-5910(97)03212-9
Oyama Y., Studies on mixing of binary system of two size by ball mill motion, Scientific Papers of the Institute of Physical and Chemical Research, 951 (1940) 17–29.
Paredes J., Shahidzadeh-Bonn N., Bonn D., Shear banding in thixotropic and normal emulsions, Journal of Physics: Condensed Matter, 23(28) (2011) 284116. https://doi.org/10.1088/0953-8984/23/28/284116
Parrella L., Barletta D., Boerefijn R., Poletto M., Comparison between a uniaxial compaction tester and a shear tester for the characterization of powder flowability, KONA Powder and Particle Journal, 26 (2008) 178–189. https://doi.org/10.14356/kona.2008016
Peshkov A., Teitel S., Universality of stress-anisotropic and stress-isotropic jamming of frictionless spheres in three dimensions: uniaxial versus isotropic compression, Physical Review E, 105(2) (2022) 24902. https://doi.org/10.1103/PhysRevE.105.024902
Poelma C., Measurement in opaque flows: a review of measurement techniques for dispersed multiphase flows, Acta Mechanica, 231(6) (2020) 2089–2111. https://doi.org/10.1007/s00707-020-02683-x
Pongó T., Fan B., Hernández-Delfin D., Török J., Stannarius R., Hidalgo R.C., Börzsönyi T., The role of the particle aspect ratio in the discharge of a narrow silo, New Journal of Physics, 24(10) (2022) 103036. https://doi.org/10.1088/1367-2630/ac9923
Preud'homme N., Opsomer E., Vandewalle N., Lumay G., Effect of grain shape on the dynamics of granular materials in 2D rotating drum,

EPJ Web of Conferences, 249 (2021) 6002. https://doi.org/10.1051/epjconf/202124906002
Rathee V., Arora S., Blair D.L., Urbach J.S., Sood A.K., Ganapathy R., Role of particle orientational order during shear thickening in suspensions of colloidal rods, Physical Review E, 101(4) (2020) 40601. https://doi.org/10.1103/PhysRevE.101.040601
Reddy R.K., Sathe M.J., Joshi J.B., Nandakumar K., Evans G.M., Recent developments in experimental (PIV) and numerical (DNS) investigation of solid–liquid fluidized beds, Chemical Engineering Science, 92 (2013) 1–12. https://doi.org/10.1016/j.ces.2012.11.017
Salehi H., Barletta D., Poletto M., A comparison between powder flow property testers, Particuology, 32 (2017) 10–20. https://doi.org/10.1016/j.partic.2016.08.003
Sarno L., Tai Y.-C., Carravetta A., Martino R., Papa M.N., Kuo C.-Y., Challenges and improvements in applying a particle image velocimetry (PIV) approach to granular flows, Journal of Physics: Conference Series, 1249 (2019) 12011. https://doi.org/10.1088/1742-6596/1249/1/012011
Sather L.J., Roth E.J., Neupauer R.M., Crimaldi J.P., Mays D.C., Experiments and simulations on plume spreading by engineered injection and extraction in refractive index matched porous media, Water Resources Research, 59(2) (2023) e2022WR032943. https://doi.org/10.1029/2022WR032943
Satone H., Iimura K., Teraoka T., Hanafusa T., Hisatani S., Nishiwaki M., Suzuki M., Analysis of granule fracture under biaxial compression, Ceramics International, 43(18) (2017) 16835–16842. https://doi.org/10.1016/j.ceramint.2017.09.081
Schnaid F., Prietto P.D.M., Consoli N.C., Characterization of cemented sand in triaxial compression, Journal of Geotechnical and Geoenvironmental Engineering, 127(10) (2001) 857–868. https://doi.org/10.1061/(ASCE)1090-0241(2001)127:10(857)
Schulze D., Powders and Bulk Solids: Behaviour, Characterization, Storage and Flow, Springer, 2008, ISBN: 9783540737674. https://doi.org/10.1007/978-3-540-73768-1
Schulze D., Round robin test on ring shear testers, Advanced Powder Technology, 22(2) (2011) 197–202. https://doi.org/10.1016/j.apt.2010.10.015
Schulze D., Discussion of testers and test procedures, in: Schulze D. (Ed.), Powders and Bulk Solids: Behavior, Characterization, Storage and Flow, 2021, pp. 187–234, ISBN: 9783030767198. https://doi.org/10.1007/978-3-030-76720-4_6
Schwedes J., Review on testers for measuring flow properties of bulk solids, Granular Matter, 5 (2003) 1–43. https://doi.org/10.1007/s10035-002-0124-4
Serial M.R., Arnaudov L.N., Stoyanov S., Dijksman J.A., Terenzi C., van Duynhoven J.P.M., Non-invasive rheo-MRI study of egg yolk-stabilized emulsions: yield stress decay and protein release, Molecules, 27(10) (2022) 3070. https://doi.org/10.3390/molecules27103070
Serial M.R., Bonn D., Huppertz T., Dijksman J.A., van der Gucht J., Van Duynhoven J.P.M., Terenzi C., Nonlocal effects in the shear banding of a thixotropic yield stress fluid, Physical Review Fluids, 6(11) (2021) 113301. https://doi.org/10.1103/PhysRevFluids.6.113301
Serial M.R., Nikolaeva T., Vergeldt F.J., Van Duynhoven J.P.M., Van As H., Selective oil-phase rheo-MRI velocity profiles to monitor heterogeneous flow behavior of oil/water food emulsions, Magnetic Resonance in Chemistry, 57 (2019) 766–770. https://doi.org/10.1002/mrc.4811
Shaebani M.R., Török J., Maleki M., Madani M., Harrington M., Rice A., Losert W., Gravity governs shear localization in confined dense granular flows, Physical Review Letters, 127(27) (2021) 278003. https://doi.org/10.1103/PhysRevLett.127.278003
Shah R.B., Tawakkul M.A., Khan M.A., Comparative evaluation of flow for pharmaceutical powders and granules, AAPS PharmSciTech, 9 (2008) 250–258. https://doi.org/10.1208/s12249-008-9046-8
Shi H., Mohanty R., Chakravarty S., Cabiscol R., Morgeneyer M., Zetzener H., Ooi J.Y., Kwade A., Luding S., Magnanimo V., Effect of particle size and cohesion on powder yielding and flow, KONA Powder and Particle Journal, 35 (2018) 226–250. https://doi.org/10.14356/kona.2018014
Shi S., Bai W., Xuan T., Zhou T., Dong G., Xie R.-J., In situ inkjet printing patterned lead halide perovskite quantum dot color conversion films by using cheap and eco-friendly aqueous inks, Small Methods, 5(3) (2021) 2000889. https://doi.org/10.1002/smtd.202000889
Shinohara K., Oida M., Golman B., Effect of particle shape on angle of internal friction by triaxial compression test, Powder Technology, 107(1–2) (2000) 131–136. https://doi.org/10.1016/S0032-5910(99)00179-5
Simons T.A.H., Weiler R., Strege S., Bensmann S., Schilling M., Kwade A., A ring shear tester as calibration experiment for DEM simulations in agitated mixers–a sensitivity study, Procedia Engineering, 102 (2015) 741–748. https://doi.org/10.1016/j.proeng.2015.01.178
Singh A., Magnanimo V., Saitoh K., Luding S., Effect of cohesion on shear banding in quasistatic granular materials, Physical Review E, 90(2) (2014) 22202. https://doi.org/10.1103/PhysRevE.90.022202
Sleiman H.C., Tengattini A., Briffaut M., Huet B., Dal Pont S., Simultaneous X-ray and neutron 4D tomographic study of drying-driven hydro-mechanical behavior of cement-based materials at moderate temperatures, Cement and Concrete Research, 147 (2021) 106503. https://doi.org/10.1016/j.cemconres.2021.106503
Stannarius R., Magnetic resonance imaging of granular materials, Review of Scientific Instruments, 88(5) (2017) 51806. https://doi.org/10.1063/1.4983135
Stannarius R., Martinez D.S., Börzsönyi T., Bieberle M., Barthel F., Hampel U., High-speed X-ray tomography of silo discharge, New Journal of Physics, 21(11) (2019a) 113054. https://doi.org/10.1088/1367-2630/ab5893
Stannarius R., Sancho Martinez D., Finger T., Somfai E., Börzsönyi T., Packing and flow profiles of soft grains in 3D silos reconstructed with X-ray computed tomography, Granular Matter, 21 (2019b) 1–10. https://doi.org/10.1007/s10035-019-0910-x
Sun C.C., Quantifying effects of moisture content on flow properties of microcrystalline cellulose using a ring shear tester, Powder Technology, 289 (2016) 104–108. https://doi.org/10.1016/j.powtec.2015.11.044
Szabó B., Török J., Somfai E., Wegner S., Stannarius R., Böse A., Rose G., Angenstein F., Börzsönyi T., Evolution of shear zones in granular materials, Physical Review E, 90 (2014) 32205. https://doi.org/10.1103/PhysRevE.90.032205
Tay J.Y.S., Liew C.V., Heng P.W.S., Powder flow testing: judicious choice of test methods, AAPS PharmSciTech, 18 (2017) 1843–1854. https://doi.org/10.1208/s12249-016-0655-3
Tegzes P., Vicsek T., Schiffer P., Avalanche dynamics in wet granular materials, Physical Review Letters, 89(9) (2002) 94301. https://doi.org/10.1103/PhysRevLett.89.094301
Tsai J.-C., Chou M.-R., Huang P.-C., Fei H.-T., Huang J.-R., Soft granular particles sheared at a controlled volume: rate-dependent dynamics and the solid–fluid transition, Soft Matter, 16(32) (2020) 7535–7543. https://doi.org/10.1039/D0SM00405G
Unger T., Török J., Kertész J., Wolf D.E., Shear band formation in granular media as a variational problem, Physical Review Letters, 92(21) (2004) 214301. https://doi.org/10.1103/PhysRevLett.92.214301
Vego I., Benders R.T., Tengattini A., Vergeldt F.J., Dijksman J.A., van Duynhoven J.P.M., Heterogeneous swelling of couscous particles exposed to a high relative humidity air, as revealed by TD-NMR and X-ray tomography, Food Structure, (2023a) 100330. https://doi.org/10.1016/j.foostr.2023.100330
Vego I., Tengattini A., Andò E., Lenoir N., Viggiani G., The effect of high relative humidity on a network of water-sensitive particles (couscous) as revealed by in situ X-ray tomography, Soft Matter, 18(25) (2022) 4747–4755. https://doi.org/10.1039/D2SM00322H
Vego I., Tengattini A., Lenoir N., Viggiani G., The influence of water sorption on the microstructure of a hydro-sensitive granular material (couscous) deduced from simultaneous neutron and X-ray tomography, Granular Matter, 25(4) (2023b) 1–14. https://doi.org/10.1007/s10035-023-01356-5
Verma A., Chauhan G., Baruah P.P., Ojha K., Morphology, rheology, and kinetics of nanosilica stabilized gelled foam fluid for hydraulic fracturing application, Industrial & Engineering Chemistry Research, 57(40) (2018) 13449–13462. https://doi.org/10.1021/acs.iecr.8b04044

Vu T.-L., Nezamabadi S., Mora S., Effects of particle compressibility on structural and mechanical properties of compressed soft granular materials, Journal of the Mechanics and Physics of Solids, 146 (2021) 104201. https://doi.org/10.1016/j.jmps.2020.104201

Wang B.-D., Song J., Li R., Han R., Zheng G., Yang H. A novel particle tracking velocimetry method for complex granular flow field, Chinese Physics B, 29(1) (2019) 14207. https://doi.org/10.1088/1674-1056/ab5936

Wang C., Song S., Gunawardana C.A., Sun D.J., Sun C.C. Effects of shear cell size on flowability of powders measured using a ring shear tester, Powder Technology, 396 (2022) 555–564. https://doi.org/10.1016/j.powtec.2021.11.015

Wang J., Fan B., Pongó T., Harth K., Trittel T., Stannarius R., Illig M., Börzsönyi T., Hidalgo R.C., Silo discharge of mixtures of soft and rigid grains, Soft Matter, 17(16) (2021) 4282–4295. https://doi.org/10.1039/D0SM01887B

Wang J., Farmani Z., Dijksman J.A., Lübeck C., Speck O., Stannarius R., Characterization of shear zones in soft granular beds by means of a novel magnetic resonance imaging technique, Granular Matter, 24(4) (2022a) 103. https://doi.org/10.1007/s10035-022-01271-1

Wang J., Harth K., Puzyrev D., Stannarius R., The effect of obstacles near a silo outlet on the discharge of soft spheres, New Journal of Physics, 24(9) (2022b) 93010. https://doi.org/10.1088/1367-2630/ac8bea

Wang L., Zheng Z., Yu Y., Liu T., Zhang Z., Determination of the energetic coefficient of restitution of maize grain based on laboratory experiments and DEM simulations, Powder Technology, 362 (2020) 645–658. https://doi.org/10.1016/j.powtec.2019.12.024

Wang Y., Snee R.D., Meng W., Muzzio F.J., Predicting flow behavior of pharmaceutical blends using shear cell methodology: a quality by design approach, Powder Technology, 294 (2016) 22–29. https://doi.org/10.1016/j.powtec.2016.01.019

Wiebicke M., Andò E., Viggiani G., Herle I. Measuring the evolution of contact fabric in shear bands with X-ray tomography, Acta Geotechnica, 15(1) (2020) 79–93. https://doi.org/10.1007/s11440-019-00869-9

Withers P.J., Bouman C., Carmignato S., Cnudde V., Grimaldi D., Hagen C.K., Maire E., Manley M., Du Plessis A., Stock S.R., X-ray computed tomography, Nature Reviews Methods Primers, 1 (2021) 18. https://doi.org/10.1038/s43586-021-00015-4

Xiu W.Z., Li R., Chen Q., Sun Q.C., Zivkovic V., Yang H., Binary-size granules segregation from core pattern to streak pattern in a rotating drum, Powder Technology, 380 (2021) 518–525. https://doi.org/10.1016/j.powtec.2020.11.035

Yang R.Y., Yu A.B., McElroy L., Bao J., Numerical simulation of particle dynamics in different flow regimes in a rotating drum, Powder Technology, 188(2) (2008) 170–177. https://doi.org/10.1016/j.powtec.2008.04.081

Zafar U., Vivacqua V., Hassanpour A., Raso G., Marigo M., Applications and case studies, in: A Hassanpour, C Hare, M Pasha (Eds.), Powder Flow: Theory, Characterisation and Application, 2019, pp. 177–208, ISBN: 9781788012249. https://doi.org/10.1039/9781788016100-00177

Zhang W., Zhao D., Dong Z., Li J., Zhang B., Yu W., The consistency factor and the viscosity exponent of soybean-protein-isolate/wheat-gluten/corn-starch blends by using a capillary rheometry, Molecules, 27(19) (2022) 6693. https://doi.org/10.3390/molecules27196693

Authors' Short Biographies

Zohreh Farmani is a PhD candidate in the Soft Matter group at the University of Amsterdam, Institute of Physics since December 2022, having previously conducted three years of research at Wageningen University (NL). Her research focuses on granular material rheology, designing experiments to understand their flow behavior. Her aim is to utilize 3D imaging to calibrate numerical methods and link microscopic details to collective mechanical behavior. She holds an MSc and BSc in Chemical and Petroleum Engineering from Persian Gulf and Shiraz Universities in Iran, with a focus on fluid dynamics in porous media.

Dr. Jan Wieringa obtained his PhD in Physics from Delft University of Technology. Since then, he mostly worked at Unilever in several R&D functions, mostly for food applications. His expertise area is primarily process science and the interaction between process and product properties.

Prof. Dr. John van Duynhoven obtained his PhD in Biophysical Chemistry and then worked as Assistant Professor and NMR facility manager at Twente University. He later switched to Unilever R&D (The Netherlands), where he led the Spectroscopy and Imaging expertise team. In his industrial career he has been involved in a wide range of industrial food research and technology projects, being responsible for development and deployment of advanced measurement techniques. In this area he also managed a wide range of academic-industrial research collaborations. Since 2010 he has held a Part-time Professorship at Wageningen University, supervising PhD students in development and application of advanced analytical methods in food and nutritional sciences.

Dr. Joshua Dijksman obtained his PhD in Physics from Leiden University and worked at Duke University (USA) as postdoctoral scholar. He held assistant and associate professor positions in the Physical Chemistry and Soft Matter group at Wageningen University. Since 2022, he is Associate Professor at the University of Amsterdam, in the Soft Matter group of the Van der Waals-Zeeman Institute, at the Institute of Physics.